

REGULATION OF BIOFILM FORMATION AND NORSPERMIDINE PRODUCTION
BY IRON IN *VIBRIO CHOLERAE*

A Thesis
by
WILLIAM PAUL BRENNAN III

Submitted to the Graduate School
at Appalachian State University
in partial fulfillment of the requirements for the degree of
MASTER OF SCIENCE

August 2015
Department of Biology

REGULATION OF BIOFILM FORMATION AND NORSPERMIDINE PRODUCTION
BY IRON IN *VIBRIO CHOLERAE*

A Thesis
by
WILLIAM PAUL BRENNAN III
August 2015

APPROVED BY:

Dr. Ece Karatan
Chairperson, Thesis Committee

Dr. Theodore Zerucha
Member, Thesis Committee

Dr. Sarah Marshburn
Member, Thesis Committee

Dr. Susan Edwards
Chairperson, Department of Biology

Max C. Poole, Ph.D.
Dean, Cratis D. Williams School of Graduate Studies

Copyright by William Paul Brennan III 2015
All Rights Reserved

Abstract

REGULATION OF BIOFILM FORMATION AND NORSPERMIDINE PRODUCTION BY IRON IN *VIBRIO CHOLERAE*

William Paul Brennan III
B.S., Appalachian State University
M.S., Appalachian State University

Chairperson: Ece Karatan

Vibrio cholerae exists in one of two states, a planktonic, or motile state, or a multicellular community known as a biofilm. The switch between these two life styles is regulated by the intracellular pool of the bacterial second messenger c-di-GMP, which is regulated by environmental signals. The polyamine norspermidine is one such signal that has been shown to promote biofilm formation. Iron availability has also been shown to regulate biofilm formation, with iron starvation decreasing biofilm growth. In addition to upregulating biofilm formation, norspermidine also forms the backbone of the siderophore, vibriobactin. Since norspermidine is involved in vibriobactin-mediated iron uptake and increases biofilm formation, this suggests a potential link between norspermidine synthesis and biofilm formation by iron availability.

The objective of this study was to determine if inhibition of vibriobactin synthesis and uptake impacts biofilm formation. Through this work I have shown that iron availability and inhibition of vibriobactin synthesis have opposite effects on biofilm formation. Iron-depletion significantly inhibits biofilm formation in wild-type *V. cholerae*, a vibriobactin

synthesis deficient mutant, a vibriobactin uptake deficient mutant, and in a vibriobactin and norspermidine synthesis deficient double mutant. While iron deficiency inhibits biofilm formation it does not regulate transcription of *vpsL* and *vpsA*, suggesting that the decrease in biofilm formation may be caused by post-transcriptional effects on exopolysaccharide synthesis, or effects on a different component of the biofilm matrix. Transcription of *nspC* and *speG* are upregulated in $\Delta vibF$ compared to wild-type and *nspC* transcription is downregulated in biofilms compared to planktonic cells, suggesting that norspermidine is being produced and accumulating and that these cells are responding to the increased levels to avoid toxicity. I have also shown that inhibition of vibriobactin synthesis leads to a significant increase in biofilm formation and changes biofilm surface morphology. My results suggest that this increase in biofilm formation is caused by accumulation of a modified, most likely acetylated, form of norspermidine in the culture media.

Acknowledgments

I would like to acknowledge the Office of Student Research and the Graduate Student Association Senate for their support of this project in the form of monetary grants for both research and travel. This project was also supported in part by NIH grant AI096358 from the National Institute of Allergy and Infectious Diseases awarded to Dr. Ece Karatan. I would like to thank Dr. Shea Tuberty and Brandon Tate, for their help with the ICP sample preparation and analysis. I would like to thank Dr. Guichuan Hou for guidance on the scanning electron microscope. I would like to thank Dr. Sarah Marshburn for all of her help with troubleshooting for my RNA work and for being a member of my committee. I would like to thank Dr. Ted Zerucha and Dr. Mary Connell for also serving on my committee. Last, but not least I would like to thank my advisor Dr. Ece Karatan. She gave me the chance to pursue a Master of Science degree and more guidance and time than I could have ever anticipated.

Dedication

I would like to dedicate this work to my parents, Bill and Mary Brennan, who have always been there for me.

Table of Contents

Abstract.....	iv
Acknowledgments.....	vi
Dedication.....	vii
List of Tables	ix
List of Figures	x
Introduction.....	1
Materials and Methods.....	11
Results.....	21
Discussion.....	45
References.....	54
Vita.....	61

List of Tables

Table 1. Bacterial Strains and Plasmids.....	12
Table 2. Primers	12

List of Figures

Fig. 1. c-di-GMP levels are regulated by environmental signals and mediate VpsR regulation of <i>vpsA-Q</i>	2
Fig. 2. Structure of the diamines putrescine and cadaverine, and the triamines spermidine and norspermidine.	3
Fig. 3. Schematic of NspS-MbaA signaling model	5
Fig. 4. Generation of free hydroxyl radicals by Fenton's reaction	5
Fig. 5. Schematic demonstrating Fur regulation of gene expression.....	6
Fig. 6. <i>V. cholerae</i> iron transport systems allow the utilization of vibriobactin, enterobactin, ferric iron, ferrous iron, ferrichrome, and heme.....	8
Fig. 7. Synthesis of oxazoline rings (A), and assembly of vibriobactin by VibF, VibB, and VibH (B)	9
Fig. 8. Vibriobactin Structure, with norspermidine backbone.....	10
Fig. 9. Colony PCR results from <i>sacB</i> counter-selectable mutagenesis of the <i>vibF</i> gene.	22
Fig. 10. Colony PCR results from <i>sacB</i> counter-selectable mutagenesis of the <i>viuA</i> gene.....	23
Fig. 11. Growth rates of WT, $\Delta vibF$, and <i>viuA::tet^r</i> in LB	24
Fig. 12. Growth rates of WT, $\Delta vibF$, and <i>viuA::tet^r</i> in LB + 100 μ g/mL EDDA.....	24
Fig. 13. Iron concentration in media extracts from wild-type, $\Delta vibF$, and <i>viuA::tet^r</i> grown in LB or LB with 100 μ g/mL EDDA, and fresh LB or LB + 100 μ g/mL EDDA as determined by ICP analysis	26
Fig. 14. Iron concentrations in cell extracts from wild-type, $\Delta vibF$, and <i>viuA::tet^r</i> grown in LB or LB with 100 μ g/mL EDDA as determined by ICP analysis	27

Fig. 15. Effect of vibriobactin synthesis (<i>ΔvibF</i>) and vibriobactin transport (<i>viuA::tet^R</i>) mutants on biofilm formation in <i>V. cholerae</i> strain MO10	28
Fig. 16. Effect of vibriobactin synthesis (<i>ΔvibF</i>) and vibriobactin transport (<i>viuA::tet^R</i>) mutants on planktonic cell growth after 24 hours in both LB and LB + EDDA	29
Fig. 17. Inhibition of vibriobactin synthesis impacts biofilm morphology as viewed by SEM at 1,200 times magnification.....	30
Fig. 18. Colony PCR results from <i>sacB</i> counter-selectable mutagenesis of the <i>vibF</i> gene in AK314 background.....	31
Fig. 19. Growth curve of wild-type and <i>ΔvibF/ΔnspC</i> in iron-replete and iron-deplete conditions.....	32
Fig. 20. Assessing biofilm formation in wild-type, a vibriobactin synthesis defective mutant (<i>ΔvibF</i>), a norspermidine defective mutant (<i>ΔnspC</i>), and a vibriobactin and norspermidine defective double mutant (<i>ΔvibF ΔnspC</i>)	33
Fig. 21. Planktonic cell growth for wild-type, a vibriobactin synthesis defective mutant (<i>ΔvibF</i>), a norspermidine defective mutant (<i>ΔnspC</i>), and a vibriobactin and norspermidine defective double mutant (<i>ΔvibF ΔnspC</i>)	34
Fig. 22. Assessing the effect of conditioned medium on wild-type and <i>ΔnspS</i> biofilm formation after 24 hours.....	36
Fig. 23. Planktonic growth for wild-type and <i>ΔnspS</i> in response to conditioned medium	37
Fig. 24. Transcript levels in wild-type and <i>ΔvibF</i> planktonic and biofilm cells.....	39
Fig. 25. Transcript levels between cells in either iron-replete or iron-deplete conditions.....	41
Fig. 26. Transcript levels in wild-type biofilm and planktonic cells compared against wild-type iron-replete transcript levels.....	43
Fig. 27. Transcript levels in <i>ΔvibF</i> planktonic and biofilm cells compared against <i>ΔvibF</i> iron-replete planktonic cells	43
Fig. 28. Transcript levels in <i>ΔvibF</i> planktonic and biofilm cells compared against wild-type planktonic and biofilm cells under the same iron conditions	44

Introduction

Vibrio cholerae is a Gram (-) pathogenic bacterium that persists in aquatic reservoirs in either a free-swimming planktonic state or in the form of a multicellular community, or biofilm (Huq *et al.*, 1990; Karatan and Watnick, 2009). This bacterium is the causative agent of the severe intestinal disease cholera, which results in voluminous diarrhea, vomiting, and if left untreated can cause severe dehydration resulting in death within 24 hours (Bomchil *et al.*, 2003). The ability to form a biofilm conveys protection to *V. cholerae* from a wide range of stressors, ranging from UV irradiation, resistance to antibiotics, and the low pH of the stomach and gastric acid barrier (Kamruzzaman *et al.*, 2010; Tamayo *et al.*, 2010). There are a wide range of potential regulators of biofilm formation, including both environmental signals and signals produced by other bacteria (Stanley and Lazazzera, 2004; Tischler and Camilli, 2004).

Biofilms are composed of many bacteria encased in self-produced exopolymeric substances (EPS), which make up the biofilm matrix, and are typically attached to some type of surface, either abiotic or biotic (Karatan and Watnick, 2009). The switch between the planktonic state and biofilm state is mediated by environmental signals, which can either be self-produced or environmental in origin. In response to a pro-biofilm signal, planktonic cells will adhere to some surface. As more planktonic cells adhere to this surface they begin to form a biofilm. Formation of a mature biofilm requires the production and excretion of *Vibrio* polysaccharide (VPS) and matrix proteins. VPS is produced by the proteins encoded

by the *vps* genes, which are clustered into two regions on the large chromosome; these two clusters are separated by the *rbm* gene cluster (Fong *et al.*, 2010). *vps* cluster I contains the genes, *vpsU* and *vpsA-K*, and the second cluster contains *vpsL-Q*, with these genes being responsible for VPS biosynthesis. The *rbm* genes *rbmC* and *rbmA*, encode for two important biofilm matrix proteins RbmC and RbmA. Expression of *vpsA-Q* is controlled in part by the transcriptional regulator VpsR, which has been shown to be under at least partial regulation by intracellular pools of the bacterial second messenger cyclic (5' to 3')-diguanosine monophosphate (c-di-GMP), which are in turn regulated by environmental signals (Fig. 1) (Tischler and Camilli, 2004). Polyamines constitute one class of environmental signals that have been shown to regulate biofilm formation in *V. cholerae*, possibly through regulation of intracellular pools of c-di-GMP (Karatan *et al.*, 2005).

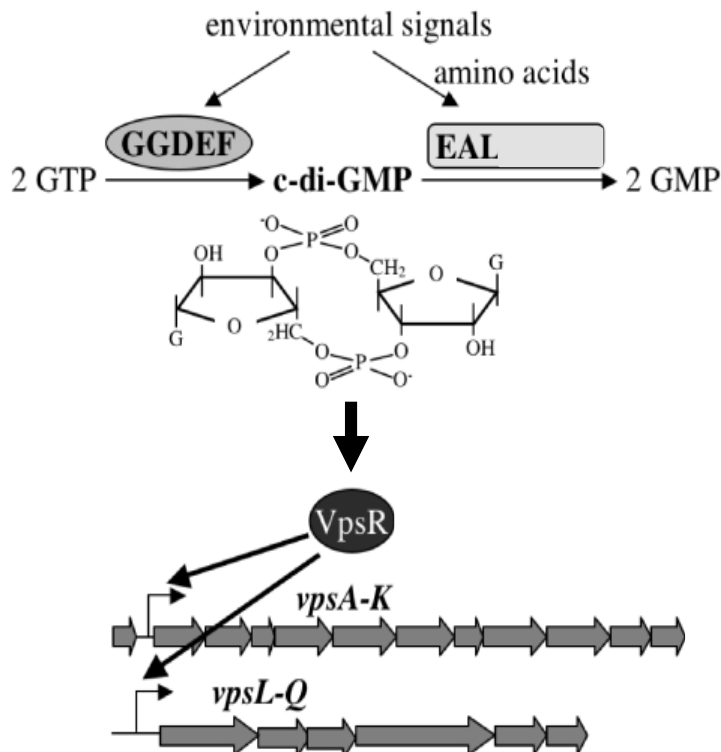


Fig. 1: c-di-GMP levels are regulated by environmental signals and mediate VpsR regulation of *vpsA-Q*. Modified from Tischler and Camilli, 2004 (Tischler and Camilli, 2004).

Polyamines are short hydrocarbon chains containing variable numbers of amine groups. They are ubiquitous in nature and are synthesized by almost all living organisms (Fig. 2) (Wortham *et al.*, 2007; Wortham *et al.*, 2010). Polyamines are synthesized and utilized by a wide range of prokaryotes (Tabor and Tabor, 1985). While some polyamines are found in a wide range of prokaryotes, like the diamine putrescine and the triamine spermidine, norspermidine, a triamine, is a rarity. Norspermidine is only synthesized by a small sub set of prokaryotes, one of which is *V. cholerae*, suggesting a potentially important role for this polyamine for this bacterium. Polyamines have been shown to be involved in a wide range of cellular processes including, cell proliferation and regulation of biofilms (Karatan *et al.*, 2005; Patel *et al.*, 2006; Lee *et al.*, 2009). Exogenous norspermidine has been shown to up regulate biofilm formation *in vitro*, suggesting that norspermidine is an important environmental signal for *V. cholerae* (Yamamoto *et al.*, 1979; Hamana and Matsuzaki, 1982; Karatan *et al.*, 2005).

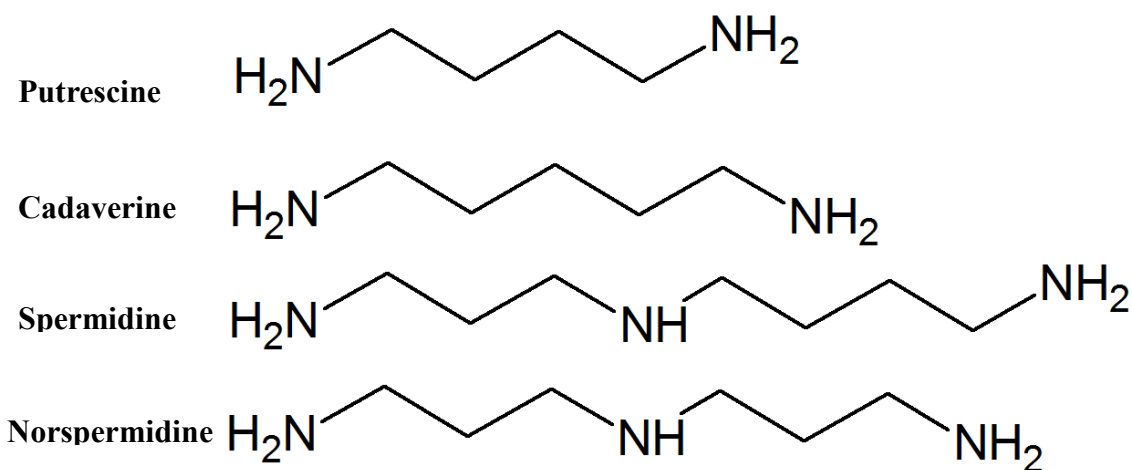


Fig. 2: Structure of the diamines putrescine and cadaverine, and the triamines spermidine and norspermidine. Structures were drawn using the ChemSketch program.

Norspermidine is believed to interact with the putative NspS/MbaA pathway and through this pathway regulate intracellular c-di-GMP levels and ultimately biofilm formation (Fig. 3) (Karatan *et al.*, 2005; Cockerell *et al.*, 2014). Cyclic-di-GMP is a bacterial second

messenger involved in regulation of sessile and motile phenotypes, with high levels corresponding with increased biofilm formation and lower levels leading to motility. Levels of c-di-GMP are regulated by synthesis from two molecules of GTP by diguanylate cyclases (DGC) containing GGDEF domains and degradation by phosphodiesterases (PDE) into either GMP by HD-GYP domains or into a linear molecule 5'-pGpG by EAL domains (Romling and Amikam, 2006). NspS is believed to bind to norspermidine present in the periplasm and once bound interacts with the periplasmic portion of the transmembrane protein MbaA. MbaA has a cytoplasmic domain containing both GGDEF and EAL domains implicating its involvement in c-di-GMP regulation. While the phosphodiesterase activity (EAL domain) of MbaA has been confirmed it is still unclear as to whether the diguanylate cyclase domain (GGDEF) is functional (Cockerell *et al.*, 2014). While this system relies on exogenous norspermidine, *V. cholerae* can also synthesize norspermidine using the enzyme carboxynorspermidine decarboxylase (NspC) produced by the gene *nspC* (Lee *et al.*, 2009; Cockerell *et al.*, 2014). In addition to being able to regulate biofilm formation, norspermidine is also used by the bacterium in the synthesis of the catecholate siderophore vibriobactin (Griffiths *et al.*, 1984).

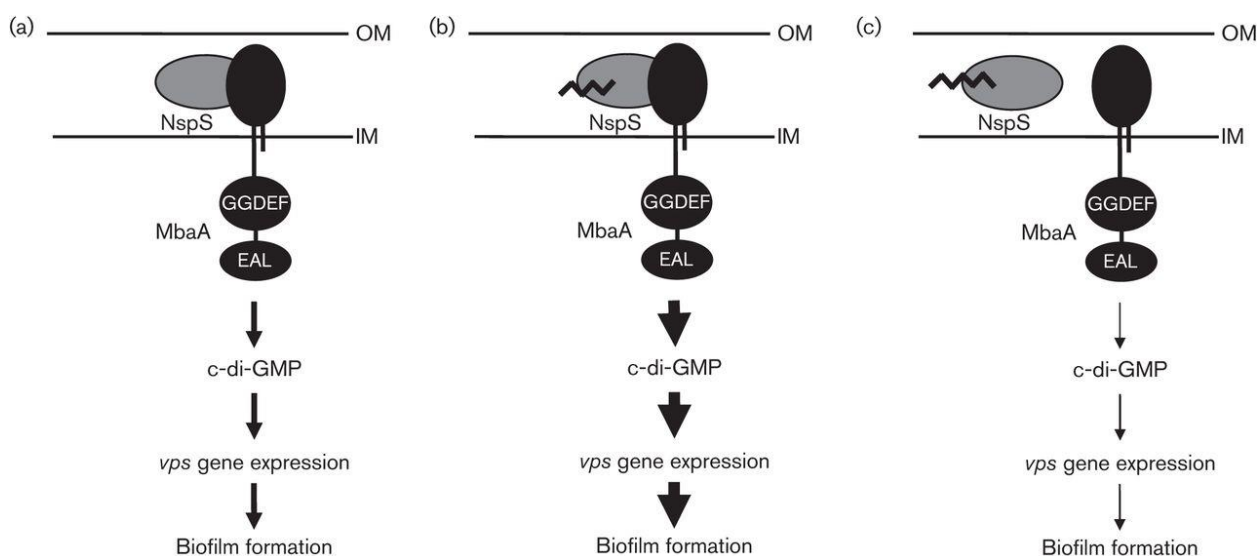


Fig. 3: Schematic of NspS-MbaA signaling model. NspS will respond to some environmental input, which regulates interaction with the inner-membrane protein MbaA, leading to regulation of intracellular c-di-GMP pools, which then impact *vps* gene expression, and ultimately biofilm formation. Model demonstrates impact of no NspS ligand (a), in the presence of norspermidine (b), and in the presence of spermidine (c). Arrow thickness demonstrates impact on c-di-GMP levels, with the thin arrow representing low c-di-GMP levels, and the thickest arrow representing highest c-di-GMP levels (Cockerell *et al.*, 2014).

Like most bacteria, *V. cholerae* requires iron for multiple cellular processes ranging from DNA metabolism to the tricarboxylic acid (TCA) cycle, which are necessary for growth and survival (Mey *et al.*, 2005b). However, if too much iron is present intracellularly this leads to a natural event known as Fenton's reaction which results in the spontaneous generation of free hydroxyl radicals (Fig. 4) (Touati, 2000). The presence of free hydroxyl radicals leads to detrimental effects in bacteria; therefore, while having too little iron impairs cell growth and function, having an excess of iron is also damaging.

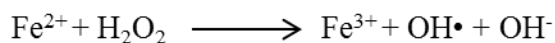


Fig. 4. Generation of free hydroxyl radicals by Fenton's reaction (Touati, 2000).

In order to maintain iron homeostasis, the transcriptional regulator Fur controls the expression of iron transport and storage related genes. Fur acts by inhibiting iron transport

pathways when there is an excess of intracellular iron, through formation of the ferri-Fur complex which will bind to the promoter of iron transport related genes, inhibiting the expression of those genes (Fig. 5) (Litwin *et al.*, 1992; Lam *et al.*, 1994; Olczak *et al.*, 2005). Fur further regulates iron homeostasis through repression of RhyB, a small regulatory RNA involved in regulation of genes encoding iron containing proteins (Mey *et al.*, 2005a; Davis *et al.*, 2005; Wyckoff *et al.*, 2007).

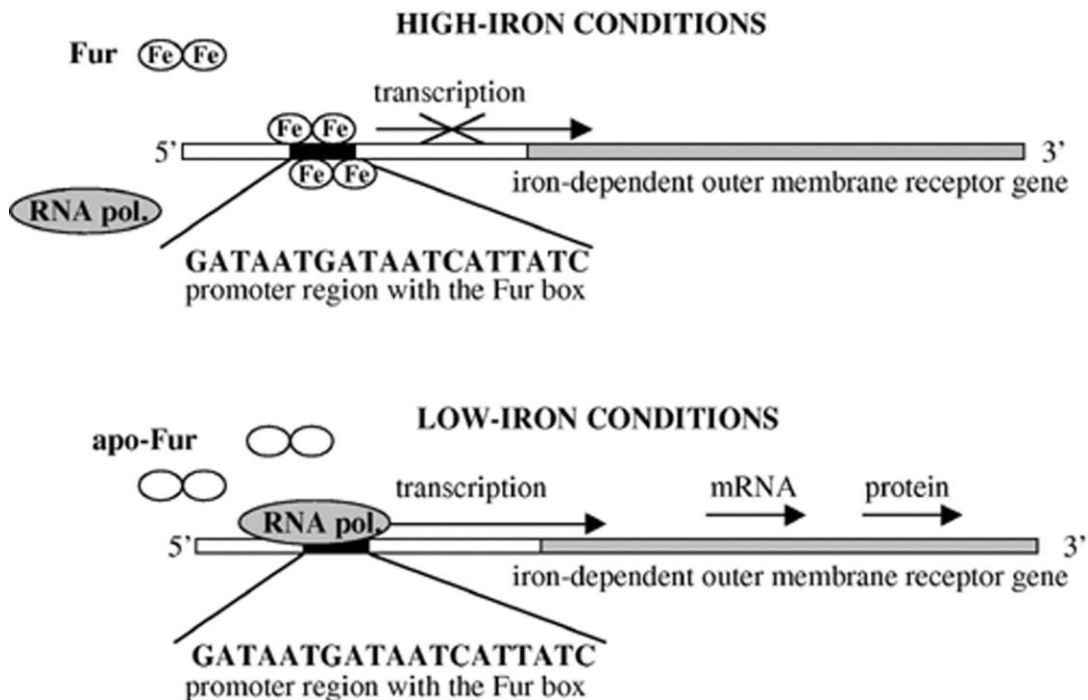


Fig. 5: Schematic demonstrating Fur regulation of gene expression. Under iron-replete conditions the Fur dimer complexes with excess iron and binds directly to the DNA at the promoter region and negatively regulates gene expression. Under iron-deplete conditions no Fur-iron complex is formed and gene transcription is not inhibited (Olczak *et al.*, 2005).

Within a host iron is known as a growth limiting factor due to the fact that not only is iron insoluble at a physiological pH, but that in total a human only has about 5 grams of iron (Doherty, 2007). Due to the insolubility of iron, the iron found in our bodies is typically bound in a protein such as lactoferrin or transferrin (Smith, 2004). *V. cholerae* like most bacteria, has multiple iron acquisition pathways through which both ferric (Fe (III)⁺) and

ferrous iron (Fe (II)^+) sources can be transported (Fig. 6) (Wyckoff *et al.*, 2006). These pathways include Fbp and Hit-mediated ferric iron transport and Sit, Efe, Vci, and Feo-mediated ferrous iron transport (Mey *et al.*, 2008; Parker Siburt *et al.*, 2012; Weaver *et al.*, 2013). In addition to these ferric and ferrous iron transport pathways, heme can be taken up directly in a TonB-dependent manner via one of two TonB systems (Occhino *et al.*, 1998; Seliger *et al.*, 2001). Alternatively, under iron stressed conditions, *V. cholerae* can either bind free iron, or “steal” the iron from host proteins like ferritin and transferrin using a siderophore, a small molecule with a high affinity for ferric iron (Butterton *et al.*, 1992). Siderophores are a versatile strategy for iron acquisition, but they are not always necessary. The iron sources present in different host environments are very specific to that host, so while siderophores might be relevant for survival in one host’s intestinal tract, a different host might have other sources of iron that are usable and sufficient for growth making siderophores irrelevant (Miethke and Marahiel, 2007). For example, under iron-limited conditions within a mouse intestine, *V. cholerae* can produce the siderophore vibriobactin, whereas in a rabbit intestine vibriobactin synthesis and transport genes are down regulated. Downregulation of siderophore related genes in the rabbit intestine suggest that some other source of iron is present, possibly heme, since heme is present in rabbit cecal fluid (Mandlik *et al.*, 2011).

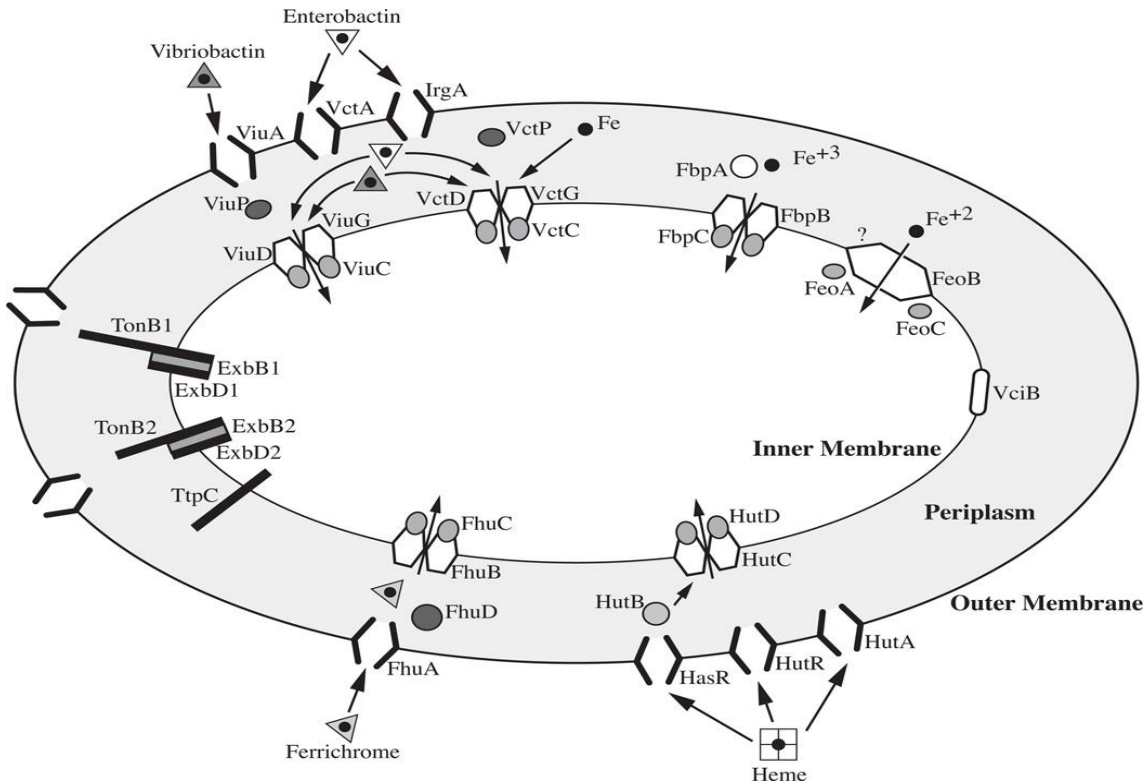


Fig. 6: *V. cholerae* iron transport systems allow the utilization of vibriobactin, enterobactin, ferric iron, ferrous iron, ferrichrome, and heme (Wyckoff and Payne, 2011).

Vibriobactin is synthesized by three proteins VibF, VibB and VibH from norspermidine, three dihydroxybenzoate (DHB) residues, and two L-threonine molecules (Wyckoff *et al.*, 2001; Marshall *et al.*, 2002; Wyckoff *et al.*, 2007). VibB and VibH act primarily as courier proteins, by bringing the vibriobactin precursors to VibF, which is responsible for attaching the oxazoline rings to the norspermidine backbone (Fig. 7 and 8). Once in the extracellular environment, vibriobactin utilizes its high affinity to bind the ferric iron bound to molecules like ferritin and lactoferrin (Griffiths *et al.*, 1984). Vibriobactin will chelate ferric iron from these molecules and bring the iron back to the cell, where it is recognized and bound by the outer membrane receptor ViuA (Butterton *et al.*, 1992). ViuA will then transport the iron-siderophore complex into the periplasm, where it is bound by a

periplasmic protein, ViuP, and eventually into the cytoplasm via the inner membrane ABC-transporter, ViuDGC, where ViuB will remove the iron from iron siderophore complex in the cytoplasm (Wyckoff *et al.*, 1999; Wyckoff *et al.*, 2007). In addition to being able to transport vibriobactin, these protein complexes can also import enterobactin, a siderophore produced by *Escherichia coli* (Wyckoff and Payne, 2011).

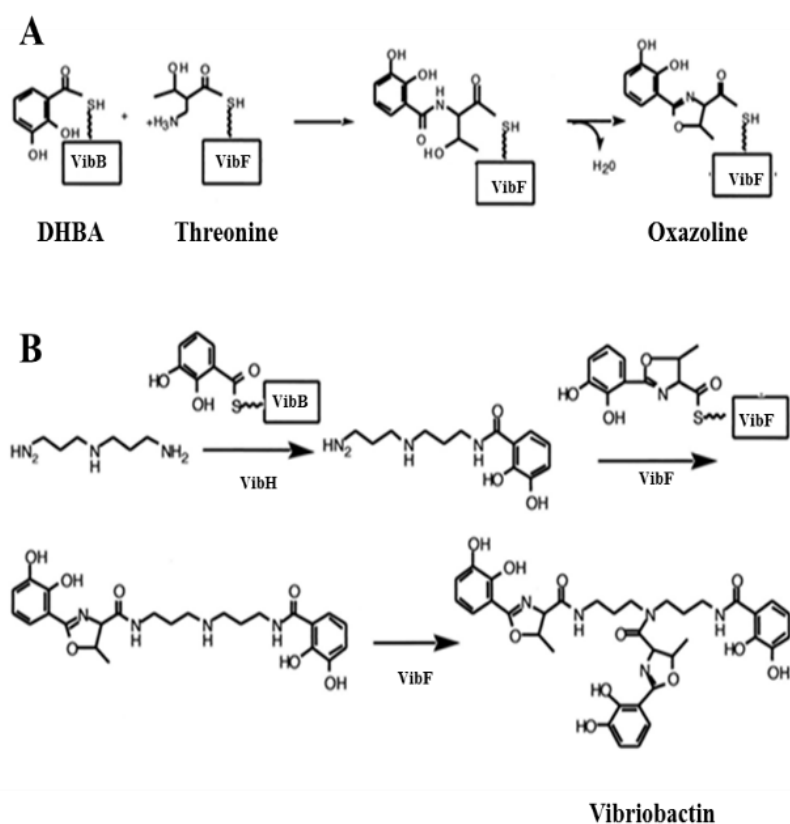


Fig. 7. Synthesis of oxazoline rings (A), and assembly of vibriobactin by VibF, VibB, and VibH (B) (Crosa and Walsh, 2002).

Since norspermidine is able to regulate biofilm formation and is required for vibriobactin synthesis, there is the potential for iron availability regulating norspermidine synthesis. While the effects of both norspermidine and iron in biofilm formation have been studied separately very little work has been directed at the potential interaction between iron and norspermidine in *V. cholerae*. This work is focusing on trying to elucidate any potential

Materials and Methods

Bacterial strains, plasmids, media and reagents

The bacterial strains and plasmids used in this study are listed in Table 1. The primers used for polymerase chain reaction (PCR) and quantitative reverse transcriptase PCR (qRT-PCR) are listed in Table 2. Primer synthesis was performed by Eurofins MWG Operon (Huntsville, AL). Bacteria were cultured in Luria-Bertani broth (LB) (1% Tryptone (Amresco, Solon, OH), 0.5% Yeast Extract (Amresco), 85 mM NaCl (Amresco)). All strains used in this study were stored at -80 °C in Luria-Bertani (LB) broth supplemented with 15% Glycerol. Frozen working strains were streaked for isolation onto LB agar plates containing relevant antibiotics. A single colony was inoculated into LB and grown overnight at 27 °C with or without the iron-specific chelator ethylenediamine-N,N'-diacetic acid (EDDA) (Sigma-Aldrich St. Louis, MO), at 100 µg/mL to create iron-starved conditions. EDDA was deferrated as described previously (Rogers, 1973). Antibiotics will be added at the following concentrations unless otherwise specified: for *V. cholerae* 100µg/mL for streptomycin (Sm) (FisherBiotech, Fair Lawn, NJ), 50µg/mL for kanamycin (Kn) (FisherBiotech), 2.5µg/mL for tetracycline (Tet) (FisherBiotech), and for *E. coli* 100µg/mL for ampicillin (Amp).

Table 1. Bacterial Strains and Plasmids

Strain/Plasmid	Genotype	Reference
<i>E. coli</i> strains		
PW298	SM10 <i>a</i> λ <i>pir</i> w/pPAC20, Amp ^r , Km ^r Tc ^r	(Miller and Mekalanos, 1988)
PW297	SM10 <i>a</i> λ <i>pir</i> pWCW3, Amp ^r Km ^r	(Miller and Mekalanos, 1988)
<i>V. cholerae</i> strains		
PW357	MO10 <i>lacZ::vpsLp</i> → <i>lacZ</i> , Sm ^r	(Haugo and Watnick, 2002)
PW249	MO10, clinical isolate of <i>V. cholerae</i> O139 from India, Sm ^r	(Waldor and Mekalanos, 1994)
PW514	MO10 <i>lacZ::vpsLp</i> → <i>lacZ</i> , Δ VIC0704, Sm ^r	
AK361	PW357 Δ <i>vibF</i> , Sm ^r	This Study
AK366	PW357 <i>viuA::tet^r</i> Sm ^r , Tc ^r	This Study
AK314	PW357 Δ <i>nspC</i> , Sm ^r	(Cockerell et al., 2014)
AK400	PW357 Δ <i>vibF</i> Δ <i>nspC</i> , Sm ^r	This Study
AK166	PW357 with <i>nspC</i>	(Parker et al., 2012)
Plasmids		
pWCW3	pCVD442 with <i>Sall-SacI</i> fragment from Pwcw2 containing 882-bp in-frame deletion of <i>vibF</i> ; Amp ^r	(Butterton et al., 2000)
pPAC20	pCVD442 with 4.2-kbp PvuII fragment containing <i>viuA::Tc^r</i> ; Amp ^r Tc ^r	(Tashima et al., 1996)
pACYC184	Km ^r Cm ^r	(Chang and Cohen, 1978)
<i>nspC</i>	pACYCY184:: <i>nspC</i>	(Parker et al., 2012)

Table 2. Primers

Primer	Description	Sequence
PCR Primers		
PA209	Forward primer for <i>vibF</i> internal deletion confirmation	5'-GTGTTGGCTGCGTTCGTGAC-3'
PA210	Reverse primer for <i>vibF</i> internal deletion confirmation	5'-GGGGTCAGTGGCATCTCCTG-3'
PA223	Forward primer for <i>viuA::Tc^r</i> confirmation	5'-CGCAAACAGCGGGTATGATC-3'
PA224	Reverse primer for <i>viuA::Tc^r</i> confirmation	5'-AAGGCTAGTCCTGCCCACTC-3'
qRT-PCR Primers		
PA259	Forward primer for <i>vpsL</i>	5'-CGCACCATAGTGAATCGCTACAT-3'
PA260	Reverse primer for <i>vpsL</i>	5'-ATTGATCTGTGCCCATCCAGTA-3'
PA261	Forward primer for <i>nspC</i>	5'-TGAAGGAGATTTCCGGGTGTGAAGA-3'
PA262	Reverse primer for <i>nspC</i>	5'-GGTTGTGCCATCCAGATAGGGTT-3'
PA263	Forward primer for <i>rpoB</i>	5'-GCCGAGATCCTGGACATCTTCTT-3'
PA264	Reverse primer for <i>rpoB</i>	5'-CGCAGTTTCACCACGCAGAC-3'
PA265	Forward primer for <i>vibF</i>	5'-GCGTTGTTGCCGTGGTTAC-3'
PA266	Reverse primer for <i>vibF</i>	5'-CGACTGCAAAGCGTATTGATG-3'
PA140	Forward primer for <i>vpsA</i>	5'-TTGCCAAGCGCTGATCAC-3'
PA141	Reverse primer for <i>vpsA</i>	5'-AGATGCACGGGATACAAAATTTG-3'
PA179	Forward primer for <i>speG</i>	5'-GCAGCGCGGAATTTCAAA-3'
PA180	Reverse primer for <i>speG</i>	5'-GGTTGATTAAGGTACGCGCAAA-3'

SacB Counter-Selectable Mutagenesis

Vibriobactin uptake and synthesis mutants and one mutant defective in vibriobactin synthesis and norspermidine synthesis were constructed using double homologous recombination and sucrose selection. The *Escherichia coli* strains PW298 and PW297 donated by Dr. Paula Watnick at Harvard University were used to create mutants defective in vibriobactin synthesis and transport. The mutant strain, AK361 was rendered defective in vibriobactin synthesis through deletion of an internal portion of the key vibriobactin synthesis gene, *vibF*, and was denoted $\Delta vibF$. Another mutant strain, AK366 was constructed through interruption of the *viuA* gene, outer membrane vibriobactin uptake protein, with a tetracycline resistance cassette, and was denoted $\Delta viuA::tet^r$. A final mutant strain, AK400, was constructed from AK314 and was defective in both vibriobactin synthesis (*vibF*) and norspermidine synthesis (*nspC*), and was denoted $\Delta vibF\Delta nspC$.

The process known as *SacB* counter-selectable mutagenesis was used to create these mutants (Miller and Mekalanos, 1988; Metcalf *et al.*, 1996). To delete the *vibF* gene, SM10 λ *pir* containing pWCW3 (donor) was mated with *V. cholerae* strain PW 357 (recipient) using LB plates without antibiotic, the mated colonies were streaked for isolation on selection agar containing 100 μ g/mL for streptomycin and 50 μ g/mL for ampicillin to select for single crossover events because *V. cholerae* has a chromosomal streptomycin marker and pWCW3 contains an ampicillin resistance marker (Table 1). This step eliminates any colonies that did not cross the pWCW3 plasmid onto the chromosome. The colonies that crossed the pWCW3 plasmid onto the chromosome were purified by streaking for isolation on selection agar with streptomycin (100 μ g/mL) and ampicillin (50 μ g/mL). Selected single colonies were streaked onto LB plates without antibiotics in order to allow for recombination

to occur within the chromosome and expel the ampicillin resistance and *SacB* genes. Multiple isolated colonies were plated onto sucrose plates (2.5 g tryptone, 1.25 g yeast extract, 3.75 g agar in 167 mL DI water, and 83 mL 30% sucrose) and allowed to incubate at room temperature for two days. Selected colonies were patched onto both ampicillin (50 μ g/mL) plates and streptomycin (100 μ g/mL) plates. Colonies that failed to grow on the ampicillin plates, but grew successfully on the streptomycin plates, were chosen for colony PCR to see if they had successfully acquired the truncated *vibF* gene. Colony PCR was performed using *vibF* specific primers (Table 2) and the PCR products were run on 1% agarose gel. Two colonies were selected containing the truncated *vibF* gene which were restreaked onto streptomycin plates to further verify they were resistant to streptomycin, grown in liquid culture and stored in LB with 15% glycerol at -80 °C.

The *viuA* mutant was constructed by mating SM10 λ *pir* containing pPAC20 with PW 357 following the *SacB* counter-selectable mutagenesis protocol used to create the *vibF* mutant (Table 1). The protocol was followed as described above with the exception that tetracycline was added at 2.5 μ g/mL to the patch plates in order to select for mutants that had acquired the tetracycline resistance cassette inserted into *viuA*. To test for mutants that had acquired the interrupted *viuA* gene, colony PCR was performed using forward and reverse primers specific to *viuA* (Table 2). Selected colonies containing the *viuA::tet^r* gene were restreaked onto plates to further verify they were resistant to tetracycline, grown in liquid culture and stored in LB with 15% glycerol at -80 °C.

The Δ *vibF*/ Δ *nspC* double mutant, was constructed by mating SM10 λ *pir* containing PAR17 with PW 357 following the *SacB* counter-selectable mutagenesis protocol used to create the *vibF* mutant (Table 1). The protocol was followed as described above with the

exception that kanamycin was added at 30 $\mu\text{g}/\text{mL}$ to the patch plates in order to select for mutants in which *nspC* had been replaced by a kanamycin resistance cassette. To test for mutants that had acquired the truncated *vibF* gene, colony PCR was performed using forward and reverse primers specific to *vibF* (Table 2). Selected colonies were streaked onto kanamycin plates (30 $\mu\text{g}/\text{mL}$) to verify kanamycin resistance, grown in liquid culture and stored in LB with 15% glycerol at $-80\text{ }^{\circ}\text{C}$.

Biofilm Assays

Biofilm formation was quantified by growing cells in glass tubes to the desired time point under the desired conditions. A single colony was used to inoculate a 2 mL LB culture and grown at 27°C for 24 hours. After 24 hours, the culture was diluted 1:50 in 2 mL fresh LB medium, grown to mid-log phase and used to inoculate three, 300 μl LB technical replicates to an OD of 0.06 and grown for 24 hours at 27°C without agitation to allow biofilm formation. After 24 hours, 150 μl of planktonic cells were carefully removed, being careful not to greatly disturb the pellicle, and placed into a 96-well microplate for optical density reading. The remaining planktonic cells were discarded. The biofilm was then washed with 300 μl 1X phosphate-buffered saline (PBS) (137 mM NaCl, 2.7 mM KCl, 10 mM Na_2HPO_4 , and 2 mM KH_2PO_4 , pH 7.4), 300 μl 1X PBS was added to the biofilm and the biofilm was homogenized by vortexing with 1.0 mm glass beads (BioSpec, Bartlesville, OK) in 1 X PBS. One hundred and fifty μl of the homogenous biofilm-PBS mixture was then added to the wells of a 96-well microplate and the biofilm and planktonic cell density was measured using a Bio-RAD microplate reader (Hercules, CA), at a wavelength of 655 nm.

Conditioned Media Biofilm Assays

A single colony was inoculated into 2 mL of LB and grown for 24 hours; after 24 hours the culture was diluted 1:50 into fresh LB and grown to mid-log phase (OD_{655} 0.5). At mid-log phase, cells were pelleted via centrifugation at 16,000 x G for 3 minutes and the media supernatant was filter sterilized using a 0.2 μ m cellulose acetate membrane (VWR, Radnor, PA). Conditioned media were mixed with fresh LB at a ratio of 2:1 and inoculated with mid-log phase cells to a starting OD_{655} of 0.06 and grown for 24 hours without agitation to allow biofilm formation. After 24 hours biofilm and planktonic cell density was measured as described above.

RNA extraction, RT-PCR, and qPCR

Biofilm samples were prepared as described previously with the exception that they were grown in 10 mL of LB. Planktonic cells were removed after 24 hrs growth and placed into a stop buffer (SB) (20 mL 5X TM buffer (50 mM tris base, 25 mM $MgCl_2$, pH 7.2), 2.5 mL 1 M sodium azide, 12.5 mL 95% EtOH with 50 mg chloramphenicol, and 80 mL nuclease free H_2O) slurry at a ratio of 1:1 (10 mL SB: 10 mL planktonic or biofilm cells) on ice. SB slurry was prepared by freezing 10 mL aliquots of SB at $-20^\circ C$, prior to use frozen SB was removed and placed on ice 10 minutes and immediately before use the SB was crushed up using a glass stir rod while being kept on ice. Biofilms were then washed with 10 mL 1X PBS and homogenized in 10 mL 1X PBS using 1.0 mm glass beads and vortexing at speed setting 6.5. Homogenized biofilm samples were then added to the 10 mL SB slurry and placed on ice. SB-treated planktonic and biofilm cells were then pelleted at 4,700 X G at $4^\circ C$ and the supernatant was discarded. Cell pellets were then frozen by immersing in a dry ice-ethanol bath and stored at $-80^\circ C$ or processed immediately. RNA was extracted from

samples by performing an initial TRIzol extraction using the TRIzol reagent (Applied Biosystems, Carlsbad, CA) and following the manufacturer's provided protocol with the following modifications: isopropanol precipitations were performed overnight and the RNA pellet was washed a second time with 100% EtOH. Following TRIzol extraction, the RNA samples were further purified with the Qiagen RNeasy Mini Kit clean up (Qiagen, Valencia, CA) using the following protocol: samples were treated with Qiagen DNase I (87.5 μ l RNA sample, 10 μ l buffer RDD, 2.5 μ l DNase I) (Qiagen) at 30°C for 30 min and then processed using the RNeasy RNA clean up protocol with one additional on-column DNase I treatment for 45 min at RT. RNA was eluted with 50 μ l nuclease free water (Applied Biosystems), and the eluate was passed through the column membrane a second time and then stored at -80°C. cDNA was prepared using the Invitrogen SuperScript VILO cDNA synthesis Kit (Applied Biosystems). qPCR reactions were performed on a 7300 Real Time PCR System (Applied Biosystems) using SYBR select master mix (Applied Biosystems) with cycle conditions of 50°C for 2 min, 95°C for 2 min, and 40 cycles of 95°C for 15 sec and 60°C for 1 min. qPCR reactions were set up at a total 20 μ l per reaction with: 10 μ l SYBR select master mix (2X), 400 nM forward and reverse primers, approximately 25 ng cDNA template, and brought up to volume with nuclease free H₂O. RNA concentration was quantified via nanodrop, using the calculated concentration approximately 2 μ g of RNA was reverse transcribed into cDNA as described previously, the assumption was made that reverse transcribing 2 μ g of RNA template would yield approximately 2 μ g of cDNA. qPCR efficiency for each primer pair was determined to be 100% +/- 10%, by creating a standard curve from the threshold cycle values of four 10-fold cDNA dilutions starting with a lowest dilution of 45 ng cDNA. Δ Ct values were calculated using the following equation: Δ Ct (sample) = (Ct (target gene) – Ct

(reference gene). $\Delta\Delta C_t$ values were calculated using the following equation: $\Delta\Delta C_t$ (target gene) = ΔC_t (treated sample) – ΔC_t (untreated sample). The ratio of the target gene in our treated sample relative to the untreated sample was determined by taking $2^{\Delta\Delta C_t}$.

ICP Analysis

In order to quantify iron levels in the media and the bacterial cells, samples were subjected to inductively coupled plasma (ICP) analysis. Twenty-four-hour cultures were diluted 1:50 into fresh media and grown to mid-log phase (OD_{655} 0.5). At mid-log phase, the cells were pelleted via centrifugation, the supernatant was removed and both the supernatant and the cell pellets were frozen until they were ready to be processed. Samples were thawed, the cell pellets were resuspended in 10 μ l/mg dH₂O, lysed by sonication (three 6 second cycles on ice, at 73% duty cycle, output control 4, on a SONICATOR W-380, QSONICA, Newton, CT), and the cellular debris precipitated via centrifugation at 16,000 X G for 10 minutes. Media samples and cellular extracts were subjected to six freeze/thaw cycles to ensure no viable cells remained. After the freeze/thaw process, 100 μ l of each sample was plated on LB plates and grown overnight to verify no live cells remained. After verifying no cells remained, samples were normalized to the smallest sample volume and then brought up to a total volume of 10 mL with dH₂O. Samples were then digested overnight in nitric acid and subjected to ICP analysis by Dr. Shea Tuberty's research group with the help of Dr. Carol Babyak. Briefly, samples were digested with 2 mL 70% Omnitrace (EMD Millipore, Billerica, MA) nitric acid following U.S. Environmental Protection Agency (EPA) Protocol 3015 with microwave assistance (MARS5Express, CEM, Matthews, NC). Following digestion, samples were filtered through Whatman 110 filter paper (GE Healthcare, Pittsburgh, PA) and brought up to a final volume of 25 mL with dH₂O. All samples were

analyzed for elemental concentration of iron (Fe) using Inductively Coupled Plasma-Optical Emission Spectrometry (ICP-OES, Varian 710 ES) by EPA Protocol SW-846 Method 6010C (EPA, 2011).

Microscopy

In order to determine biofilm morphology and architectural characteristics of various strains under iron replete or iron deplete conditions, Scanning Electron Microscopy (SEM) was performed on a FEI Quanta 200 Environmental Scanning Electron Microscope. Biofilms were grown on glass microscope slides submerged in a 50 mL-conical tube containing 10 mL LB, fixed with 2.5% glutaraldehyde (TCI America, Portland, OR) in 0.1M sodium phosphate buffer (pH 7), dehydrated through an ethanol gradient of 50%, 70%, 85%, 95%, 100%, 100%, with the sample equilibrating in 10 mL of each ethanol concentration for 1 hour, dried via critical point drying using a Tousimis 931 critical point dryer (Rockville, MD), mounted on SEM stubs, sputter coated using a Polaron SEM coating system (East Sussex, UK), and subjected to SEM analysis.

Extraction, benzoylation, and detection of polyamines

In order to identify and quantify polyamines, polyamines were extracted and analyzed as previously described (Morgan, 1998; McGinnis *et al.*, 2009; Parker *et al.*, 2012). Biofilms were grown as previously described, with the exception that biofilm cultures were set up in 10 mL of LB. After 24 hours growth, the planktonic cells were removed using a 5 mL serological pipette and the biofilm was washed with 1X PBS. Biofilms were then homogenized in 10 mL 1X PBS by vortexing with glass beads. Planktonic cells and biofilm cells were pelleted by centrifugation, cell pellets were washed with 1X PBS, and re-pelleted by centrifugation. Cell pellets were then resuspended in 10 µg/mL dH₂O and lysed via

sonication (three 6 second cycles on ice, at 73% duty cycle, output control 4, SONICATOR W-380) on ice. Cellular debris were pelleted out via centrifugation at 16,000 X G for 10 minutes and supernatants were collected. Total cellular protein was precipitated with 20 μ l 50% Trichloroacetic acid (TCA), and centrifuged at 16,000 X G for 1 minute. The supernatant was transferred to a clean microfuge tube and subjected to benzylation. Benzylation procedure was followed as described previously (Morgan, 1998, McGinnis *et al.*, 2009; Parker *et al.*, 2012); briefly polyamines were extracted twice with chloroform, samples were evaporated to dryness, and resuspended in 100 μ l HPLC mobile phase (60/40 ratio of methanol and water). In addition to samples a polyamine standard, containing 0.1 mM each of cadaverine, diaminopropane, putrescine, spermidine, and norspermidine, was prepared each time and benzyolated following the above procedure. All HPLC analysis was carried out on a Waters 1525 Binary Pump with a 2487 Dual Wavelength Absorbance Detector set at 254 nm and a Phenomenex Spherclone 5u ODS column (5 μ m, 250 X 4.6 mm), fitted with a 4.0 X 3.0 mm guard cartridge (Phenomenex, Torrance, CA). Runs were completed using a 45-60% methanol gradient for 30 minutes, followed by an isocratic equilibration step of 45% methanol in water for 10 minutes. Forty μ l of each sample was injected into the column followed by three 60/40 methanol washes. A polyamine standard (described above) was run first for all injection runs in order to positively identify chromatogram peaks.

Results

Verification of vibF and viuA mutants

Iron starvation has been shown to decrease biofilm formation. Based on this observation, we hypothesized that inhibition of iron uptake through the vibriobactin pathway would also lead to a decrease in biofilm formation (Mey *et al.*, 2005a). To test this hypothesis, two mutants were constructed as described previously to investigate inhibition of vibriobactin synthesis ($\Delta vibF$) and vibriobactin mediated iron uptake (*viuA::tet^r*). These mutations were constructed in a strain that has a chromosomal *vpsL* promoter fusion to the beta-galactosidase gene in order to also assess the effect of iron starvation on *vps* gene expression. Several candidates were subjected to colony PCR to verify that they had successfully crossed the truncated *vibF* gene onto the chromosome. The *vibF* primers were designed to amplify a 1,500 bp fragment of the *vibF* gene covering the portion that would be deleted in a successful mutant. A band present at 851 bp is indicative of the deletion of the 649 bp internal fragment. Lanes two, four, eight, and nine show that those colonies successfully acquired the truncated *vibF* gene, while lanes three, five, six, and seven showed that these colonies still contained the intact *vibF* gene (Fig. 9).

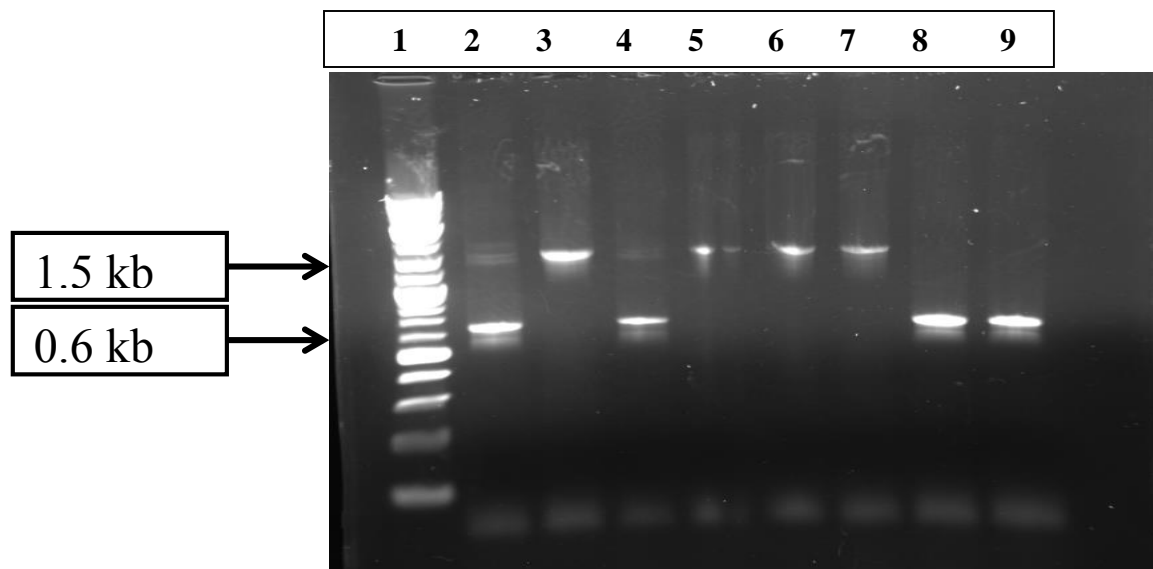


Fig. 9: Colony PCR results from *sacB* counter-selectable mutagenesis of the *vibF* gene. Lane one contains the 2-Log Kb molecular marker (NE Biolabs) with relevant bands indicated on the left. Lanes two through nine contain products of colony PCR using ampicillin sensitive colonies that could have potentially picked up the truncated *vibF* gene.

The outer-membrane vibriobactin receptor ViuA was rendered nonfunctional by inserting a tetracycline resistance cassette into the *viuA* gene. To confirm the insertion of the tetracycline cassette, primers amplifying a 700 bp region of the *viuA* gene were used. This region contains the insertion site for the 960 bp tetracycline resistance cassette, which means any colony with a 700 bp PCR product still contains the uninterrupted *viuA* gene and any colony with a 1,660 bp PCR product contains the interrupted *viuA* gene. Lanes two, three, six, and eight show that these colonies contain the *viuA* gene with the tetracycline cassette insertion, while lanes four, five, and seven did not acquire the tetracycline cassette interrupted *viuA* gene (Fig. 10).

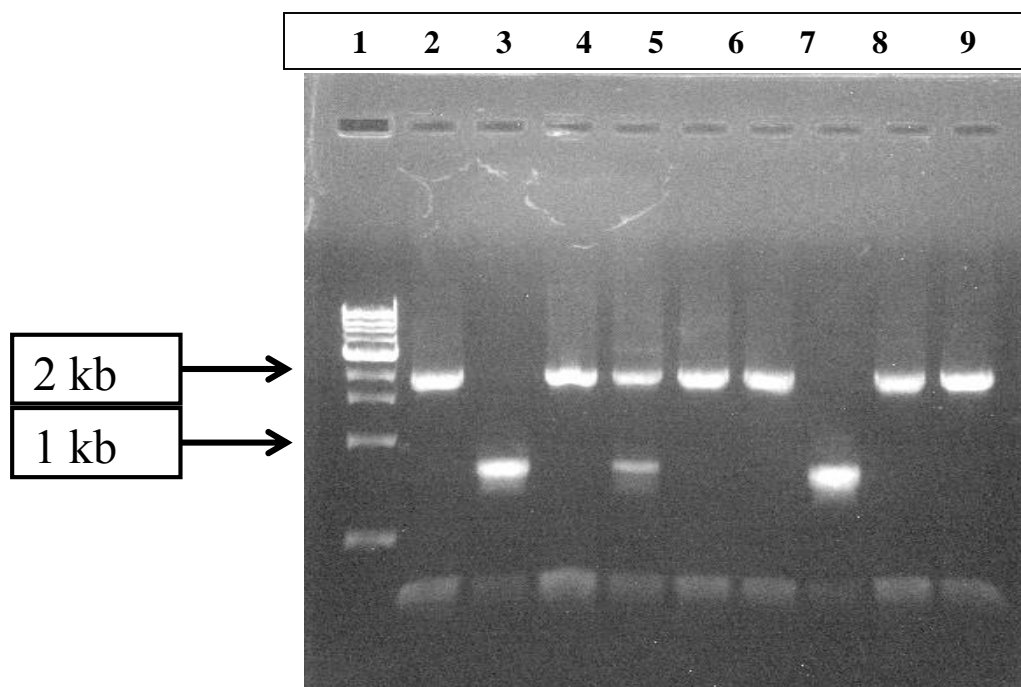


Fig. 10: Colony PCR results from *sacB* counter-selectable mutagenesis of the *viuA* gene. Lane one contains the 1 Kb molecular marker (NE Biolabs) with relevant bands indicated on the left. Lanes two through ten contain tetracycline resistant colonies that could have potentially picked up the elongated *viuA* gene.

Vibriobactin synthesis ($\Delta vibF$) and uptake (*viuA::tet^r*) mutants have wild-type planktonic growth rates regardless of iron availability

Once the mutants were constructed, growth curves were performed over 24 hours in order to verify that no growth defects were introduced in the process of generating the mutants or in response to iron deficiency through the addition of EDDA. Cell density was measured at one hour increments for the first 10 hours and then later at the 24 hour time point. Neither mutant showed any significant change in growth when compared to the isogenic wild-type strain regardless of iron availability (Fig. 11 and 12). A concentration of 100 $\mu\text{g/mL}$ of EDDA was chosen for this work because previous work has shown that this concentration inhibits biofilm growth but not planktonic growth (Mey *et al.*, 2005a).

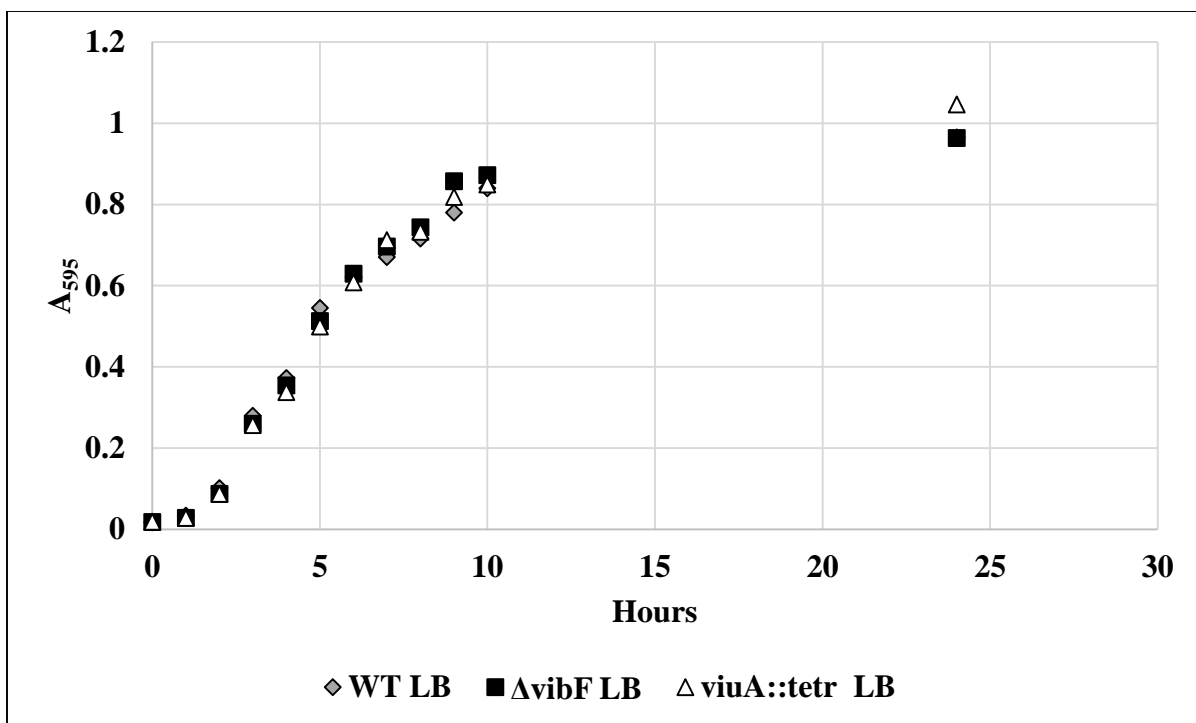


Fig. 11: Growth rates of WT, $\Delta vibF$, and $viuA::tet^r$ in LB. Y-axis represents optical density (OD_{595}) at each time point as indicated in hours on the X-axis.

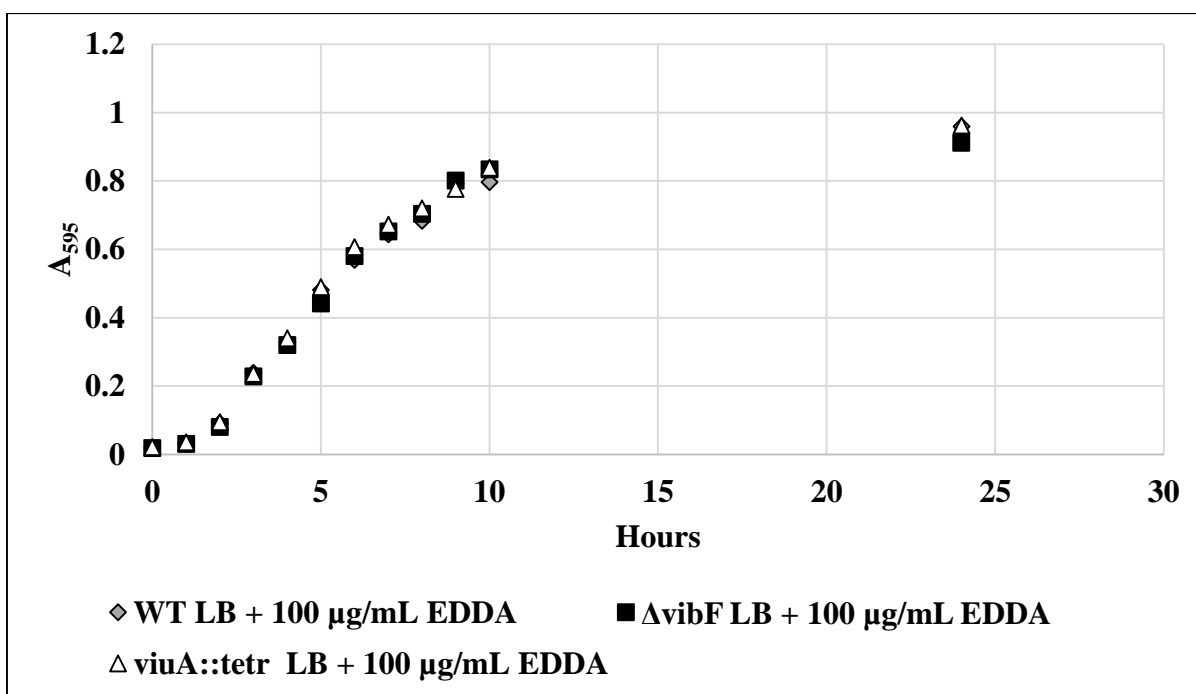


Fig. 12: Growth rates of WT, $\Delta vibF$, and $viuA::tet^r$ in LB + 100 $\mu\text{g/mL}$ EDDA. Y-axis represents optical density (A_{595}) or cell density at each time point as indicated in hours on the X-axis.

Iron concentration in cell and media extracts

Next, we wanted to determine if the cells were being starved of iron in response to addition of EDDA. Prior to treating media with EDDA it is deferrated to free any bound iron, so addition of EDDA should not add any iron to the media. In order to verify that there is no difference in iron levels between LB and LB with EDDA, fresh media and spent media iron concentrations were quantified using ICP analysis. Fresh LB with and without EDDA is expected to have identical iron concentrations, but the results showed that LB with EDDA had an iron concentration about half of LB only. The spent media should hypothetically show an increased iron concentration in LB with EDDA as EDDA should be chelating iron and making it less available to the cells and LB only should show a decrease in iron as cells can easily transport and utilize the iron. Furthermore, wild-type spent media should have a lower iron concentration in LB with EDDA compared to $\Delta vibF$ and $viuA::tet^r$ as both of these mutants are impaired in siderophore mediated iron transport whereas the wild-type has no deficiency. However, no difference may be seen in iron concentrations, as it is possible that other iron transport pathways may be sufficient for iron-uptake in both mutants. Spent media from cultures containing wild-type, $\Delta vibF$, and $viuA::tet^r$ did not show any significant differences in iron concentrations, while LB has a slightly higher iron concentration than LB with EDDA (Fig. 13).

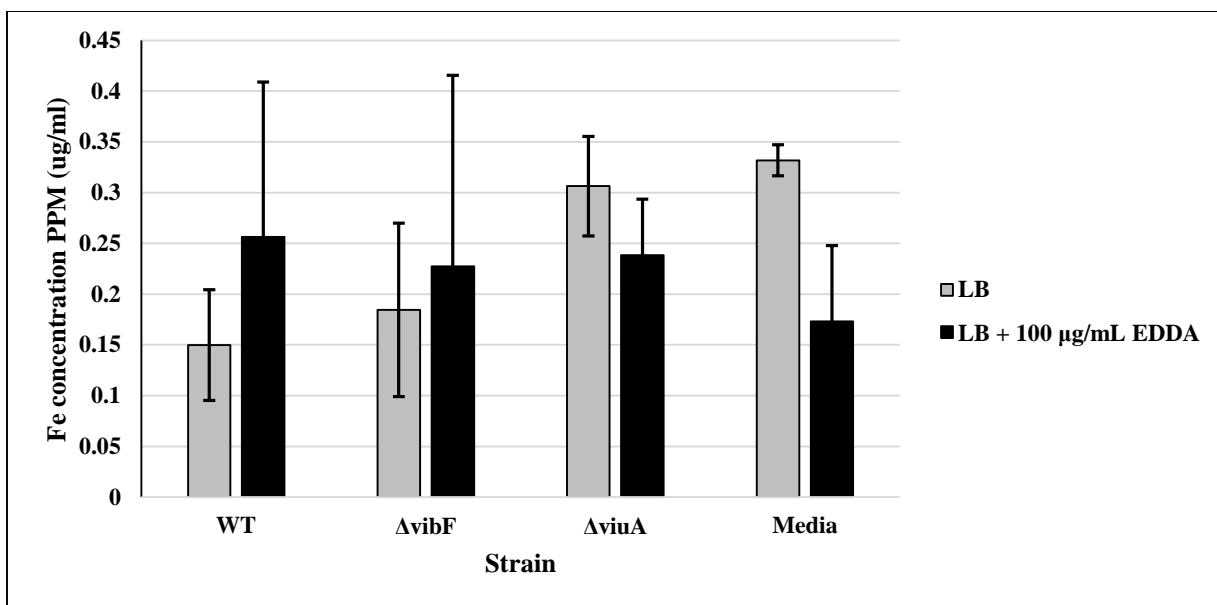


Fig. 13: Iron concentration in media extracts from wild-type, $\Delta vibF$, and $viuA::tet^r$ grown in LB or LB with 100 $\mu\text{g}/\text{mL}$ EDDA, and fresh LB or LB + 100 $\mu\text{g}/\text{mL}$ EDDA as determined by ICP analysis. Iron concentration was quantified as PPM which corresponds to $\mu\text{g}/\text{mL}$ (Y-axis) for all spent mediums as well as fresh media (X-axis). Data represents the average of three biological replicates for each condition, error bars represent standard deviation.

To determine whether the bacteria were starved of iron under various conditions, we next looked at iron concentrations in the cell extracts. ICP analysis of cell extracts from wild-type and $\Delta vibF$ showed no significant differences in iron concentrations between LB and LB with 100 $\mu\text{g}/\text{mL}$ EDDA. $viuA::tet^r$ cell extracts showed increased iron concentrations when grown in LB with EDDA compared to cell extracts grown in LB only (Fig. 14).

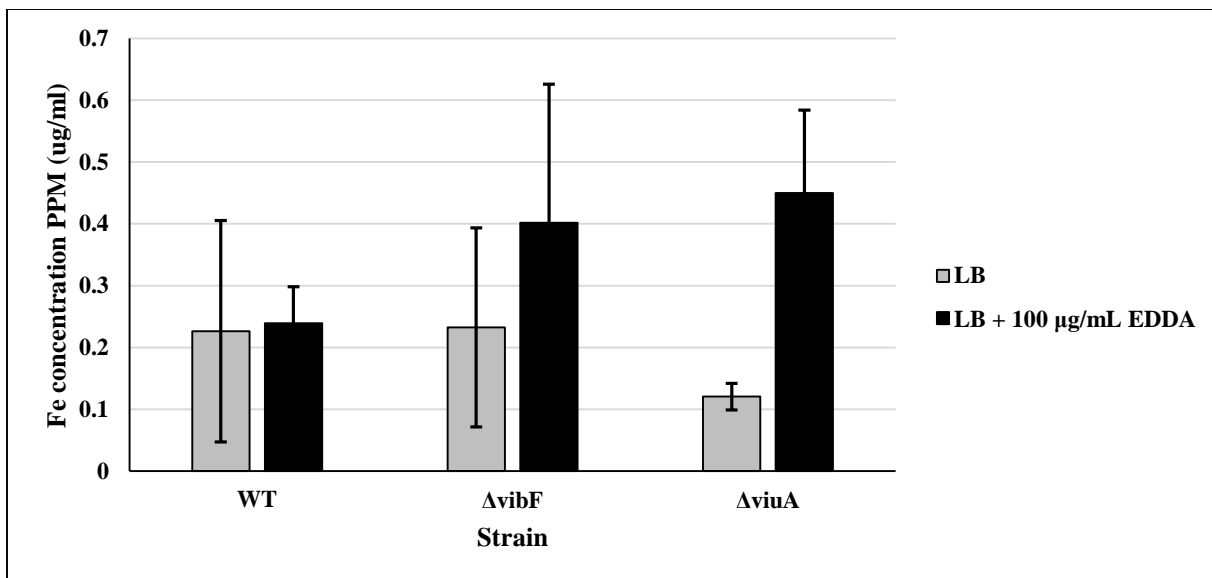


Fig. 14: Iron concentrations in cell extracts from wild-type, $\Delta vibF$, and $viuA::tet^r$ grown in LB or LB with 100 $\mu\text{g}/\text{mL}$ EDDA as determined by ICP analysis. Iron concentration was quantified as PPM which corresponds to $\mu\text{g}/\text{mL}$ (Y-axis) for all cell extracts (X-axis). Data represents the average of three biological replicates for each condition, error bars represent standard deviation.

Inability to synthesize vibriobactin increases biofilm formation

ICP analysis did not generate any clear results as to whether cells were being starved of iron; however, I proceeded to investigate the effects of addition of EDDA to LB on wild-type, $\Delta vibF$, and $viuA::tet^r$ biofilm formation. Mey et. al, showed that iron inhibition through addition of EDDA generates a decrease in biofilm formation in a concentration dependent manner (Mey *et al.*, 2005a). Based on this data, I hypothesized that the lack of vibriobactin synthesis or uptake would negatively impact biofilm formation through iron deficiency. This hypothesis was tested using biofilm assays comparing two mutants with the wild-type isogenic parental strain. A mutant defective in vibriobactin synthesis, $\Delta vibF$, was utilized to test if inhibition of vibriobactin synthesis impacts biofilm formation and a vibriobactin transport mutant, $viuA::tet^r$, was used to test if lack of vibriobactin-mediated iron transport impacts biofilm formation. Deletion of $vibF$ generated a 56-64% increase in

biofilm formation in iron-deplete and iron-replete conditions respectively. Deletion of *viuA* on the other hand had no effect on biofilm formation. For all strains tested iron deficiency created through the addition of EDDA decreased biofilm formation for that strain compared to iron-replete conditions (Fig. 15). Growth curves showed that neither the mutations nor the addition of EDDA affect total cell density; therefore planktonic cell density was quantified in each biofilm assay to confirm that differences in biofilm growth were not due to differences in total cell density. As expected planktonic cell density was higher for all strains under iron-deplete conditions compared to planktonic growth in iron-replete conditions, demonstrating that the differences in biofilm growth were not due to differences in total cell density (Fig. 16).

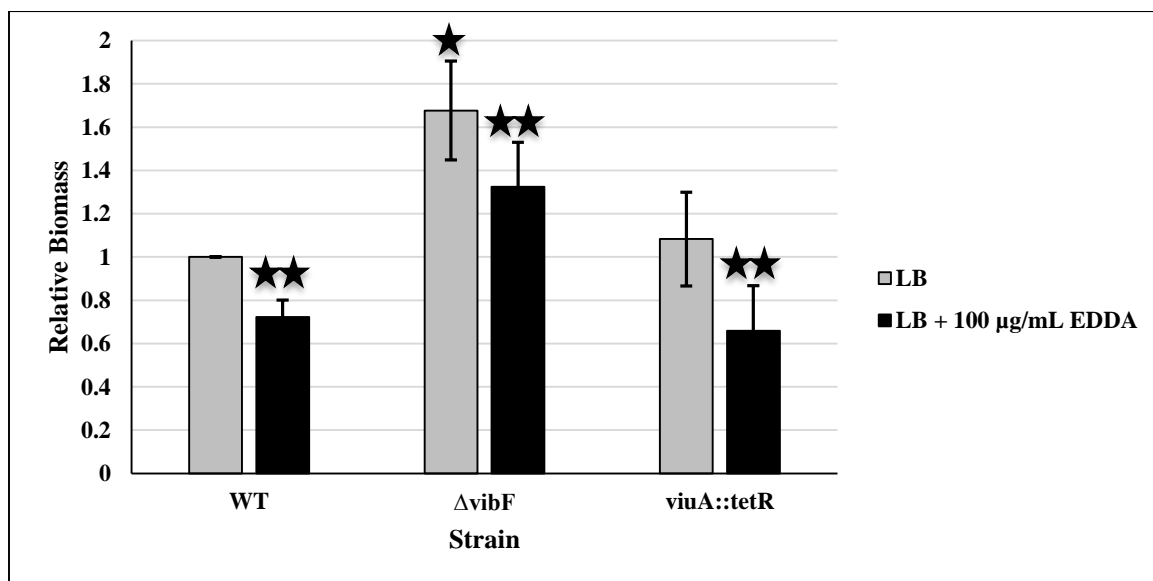


Fig. 15: Effect of vibriobactin synthesis ($\Delta vibF$) and vibriobactin transport (*viuA::tet^r*) mutants on biofilm formation in *V. cholerae* strain MO10. *V. cholerae* mutants were grown in LB as described previously and biofilm formation was quantified at 24 hours. Relative biomass was calculated using the following equation $OD_{655} \text{ mutant} / OD_{655} \text{ wild-type}$ (Y-axis). A single star indicates a statistically significant difference between that strain and wild-type. Two stars indicates a statistically significant difference between the iron-deplete biofilm growth for that strain compared to its growth in iron-replete media. A p-value <0.05 was considered significant. Data represents the average of five biological replicates for each condition, error bars represent standard deviation.

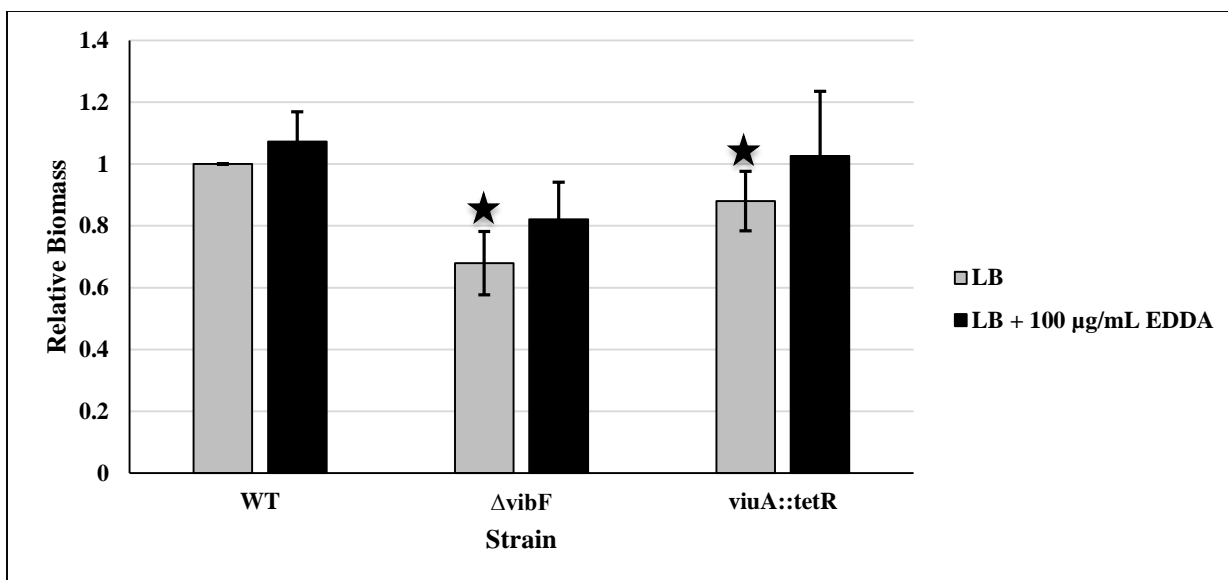


Fig. 16: Effect of vibriobactin synthesis ($\Delta vibF$) and vibriobactin transport ($viuA::tet^r$) mutants on planktonic cell growth after 24 hours in both LB and LB + EDDA. Relative biomass was calculated using the following equation $OD_{655} \text{ mutant} / OD_{655} \text{ wild-type}$ (Y-axis). A single star indicates a statistically significant difference between that strain and wild-type. A p-value < 0.05 was considered significant. Data represents the average of five biological replicates for each condition, error bars represent standard deviation.

Inability to synthesize vibriobactin impacts biofilm morphology

Inhibition of vibriobactin synthesis generated on average a 64-56% increase in biofilm growth compared to wild-type in iron-replete or iron-deplete conditions respectively. The next step was to investigate if inhibition of vibriobactin synthesis impacts biofilm morphology. Biofilms were imaged using SEM after 24 hours static growth. Wild-type biofilms formed well-ordered mushroom like macrocolonies with what appear to be water and nutrient channels regardless of iron availability. Whereas $\Delta vibF$ formed a sheet like biofilm that appears to take up more surface area on the glass slide regardless of iron availability (Fig. 17).

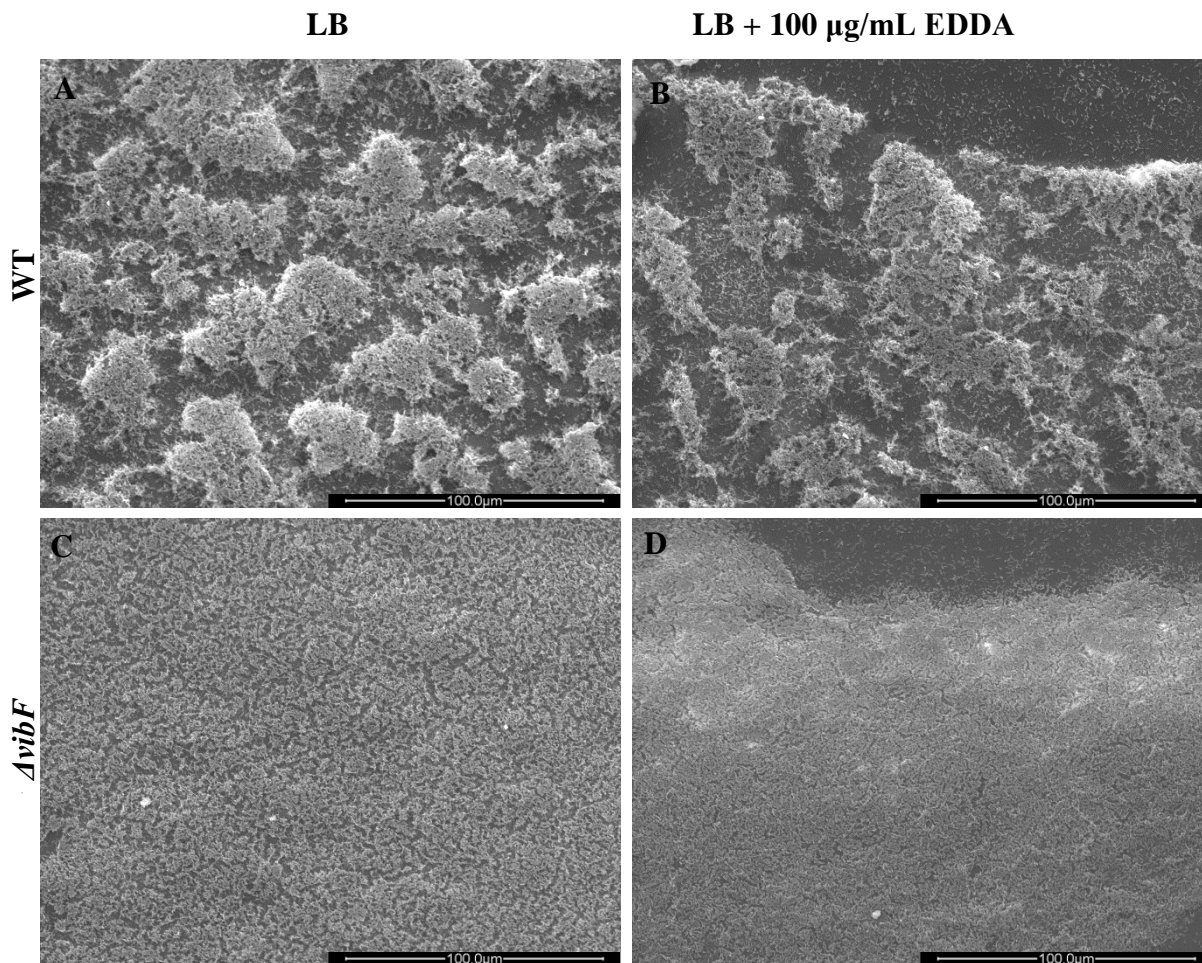


Fig. 17: Inhibition of vibriobactin synthesis impacts biofilm morphology as viewed by SEM at 1,200 times magnification. Biofilms were fixed and imaged after 24 hours growth for wild-type (WT) grown in iron-replete media (LB) (A), wild-type (WT) grown in iron-deplete media (LB + 100 $\mu\text{g}/\text{mL}$ EDDA) (B), ΔvibF grown in iron-replete media (LB) (C), and ΔvibF grown in iron-deplete media (LB + 100 $\mu\text{g}/\text{mL}$ EDDA) (D).

Construction of a $\Delta\text{vibF}/\Delta\text{nsrP}$ double mutant.

The original hypothesis of inhibition of vibriobactin synthesis or vibriobactin-mediated iron uptake leading to a decrease in biofilm formation had to be rejected due to the increase in biofilm formation in the vibriobactin synthesis mutant. To explain this increase in biofilm formation I hypothesized that lack of the VibF protein leads to the accumulation of some signal which in turn generates the increase in biofilm formation. I hypothesized that this signal could be norspermidine, as norspermidine is a component of vibriobactin, and

previous studies have demonstrated that exogenous and endogenous norspermidine affects biofilm formation in a positive manner (Karatan *et al.*, 2005; Lee *et al.*, 2009).

Norspermidine is synthesized by carboxynorspermidine decarboxylase which is encoded by the *nspC* gene. In order to test this hypothesis, I needed to construct a mutant defective in vibriobactin synthesis and norspermidine synthesis, $\Delta vibF \Delta nspC$. $\Delta vibF \Delta nspC$ was generated as described above. Several candidates were selected and verified via colony PCR. As described above, primers amplifying a 1,600 bp portion of the *vibF* gene were used to test for colonies that had crossed the truncated *vibF* gene onto the chromosome. Bands corresponding to a 851 bp fragment indicated a successful cross and the colonies in lanes four and five were frozen at -80°C (Fig. 18).

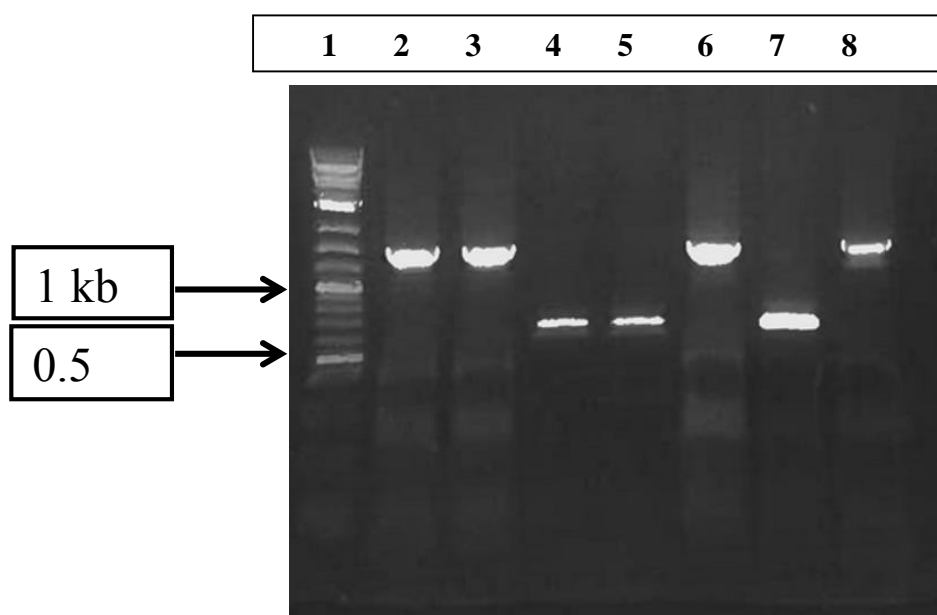


Fig. 18: Colony PCR results from *sacB* counter-selectable mutagenesis of the *vibF* gene in AK314 background. Lane one contains the 2-Log Kb molecular marker (NE Biolabs) with relevant bands indicated on the left. Lanes two through nine contain products of colony PCR using ampicillin sensitive colonies that could have potentially picked up the truncated *vibF* gene.

Mutation in nspC is epistatic over vibF in regulation of biofilm formation

The next step was to verify that no growth defects were introduced through creating the norspermidine and vibriobactin synthesis deficient double mutant. Growth was measured over 24 hours with initial measurements every hour for the first 8 hours, for both the mutant and wild-type in both iron-replete and iron-deplete conditions. The norspermidine and vibriobactin synthesis deficient double mutant lagged in growth compared to wild-type initially, but once in log phase the slope is comparable to wild-type and eventually reaches the same stationary phase cell density as wild-type (Fig. 19).

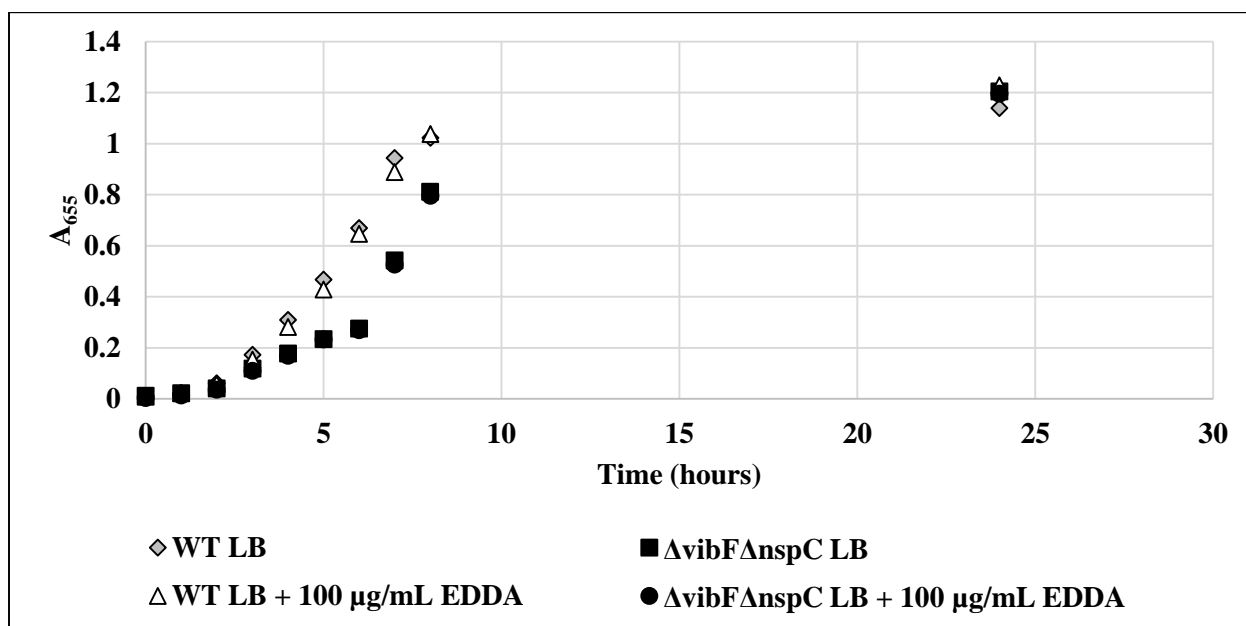


Fig. 19: Growth curve of wild-type and $\Delta vibF/\Delta nspC$ in iron-replete and iron-deplete conditions. Y-axis represents optical density (A_{595}) or cell density at each time point as indicated in hours on the X-axis.

Based on the observation that inhibition of vibriobactin synthesis generated an increase in biofilm formation, we hypothesized that this increase could be related to production and accumulation of vibriobactin precursors. To test this hypothesis two additional mutants were investigated, a mutant defective in vibriobactin and norspermidine

synthesis, and a mutant defective in norspermidine synthesis with no mutation in *vibF*. All four strains were grown in iron-replete or iron-deplete media for 24 hours under static conditions and then planktonic and biofilm growth was quantified as described previously. $\Delta vibF$ biofilm formation was consistent with a 40% increase compared to wild-type in iron-replete conditions and a 30% increase in iron-deplete conditions compared to wild-type. Both the $\Delta vibF/\Delta nspC$ double mutant and the $\Delta nspC$ mutant showed a significant decrease in biofilm growth in iron-replete conditions, with both strains producing a 40% decrease compared to wild-type. Biofilm formation was further decreased for both of these strains in iron-deplete conditions (Fig. 20). Planktonic cell growth for both the $\Delta vibF/\Delta nspC$ double mutant and the $\Delta nspC$ mutant was significantly higher than planktonic growth by either wild-type or $\Delta vibF$ (Fig. 21).

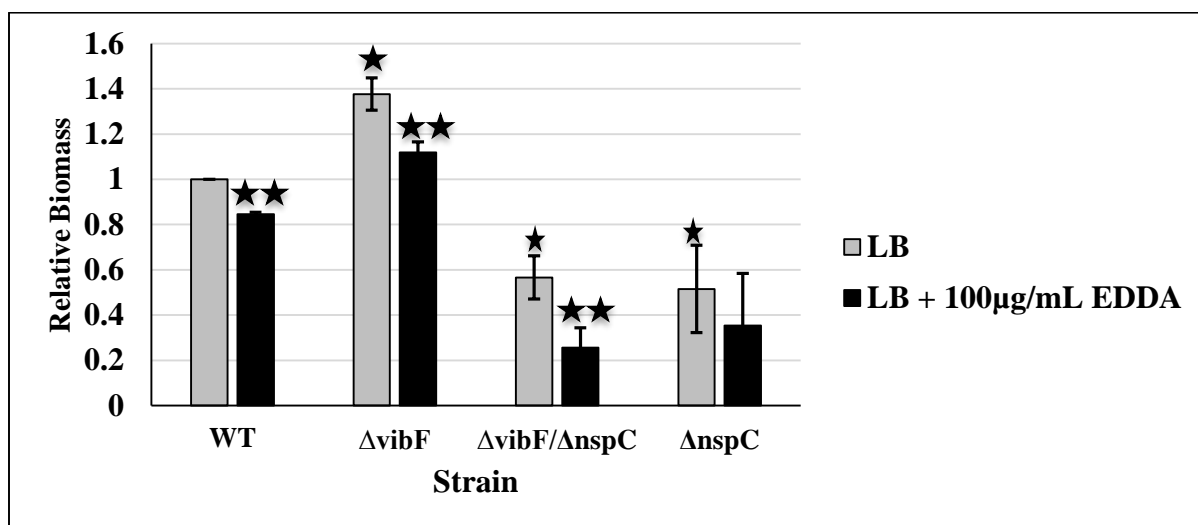


Fig. 20: Assessing biofilm formation in wild-type, a vibriobactin synthesis defective mutant ($\Delta vibF$), a norspermidine defective mutant ($\Delta nspC$), and a vibriobactin and norspermidine defective double mutant ($\Delta vibF \Delta nspC$). *V. cholerae* mutants were grown in LB as described previously and biofilm formation was quantified at 24 hours. Relative biomass was calculated using the following equation $OD_{655} \text{ mutant} / OD_{655} \text{ wildtype}$ (Y-axis). A single star indicates a statistically significant difference between that strain and wild-type. Two stars indicates a statistically significant difference between the iron-deplete biofilm growth for that strain compared to its growth in iron-replete media. A p-value < 0.05 was considered significant. Data represents the average of three biological replicates for each condition, error bars represent standard deviation.

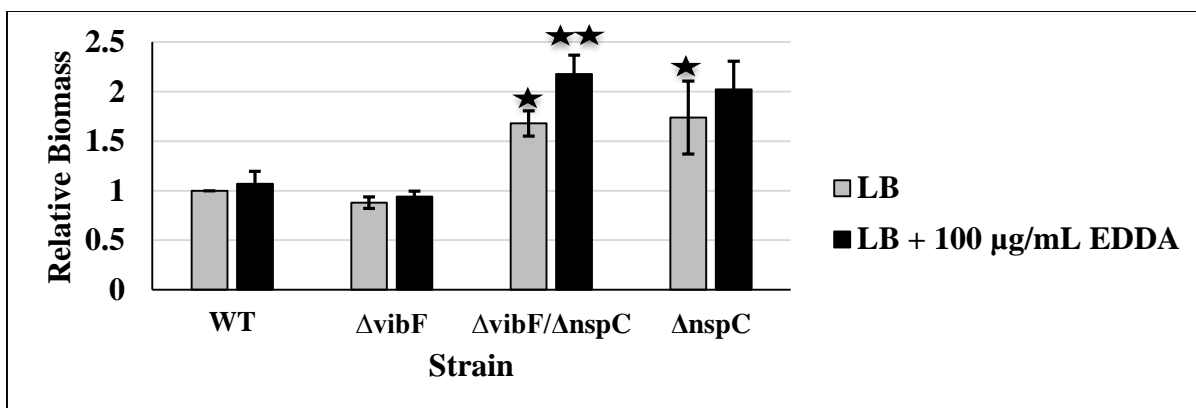


Fig. 21: Planktonic cell growth for wild-type, a vibriobactin synthesis defective mutant (*ΔvibF*), a norspermidine defective mutant (*ΔnspC*), and a vibriobactin and norspermidine defective double mutant (*ΔvibF ΔnspC*). Relative biomass was calculated using the following equation $OD_{655} \text{ mutant} / OD_{655} \text{ wild-type}$ (Y-axis). A single star indicates a statistically significant difference between that strain and wild-type. Two stars indicates a statistically significant difference between the iron-deplete biofilm growth for that strain compared to its growth in iron-replete media. A p-value <0.05 was considered significant. Data represents the average of three biological replicates for each condition, error bars represent standard deviation.

Conditioned media from *ΔvibF* and *nspC* overexpression mutant increase biofilm formation in wild-type but not *ΔnspS* mutant

Inhibition of vibriobactin synthesis generated a significant increase in biofilm formation. This increase was nullified through inhibition of norspermidine synthesis in this mutant, indicating that *nspC* is epistatic over *vibF* in regards to biofilm formation. This result is not surprising as norspermidine forms the backbone of vibriobactin and in the absence of norspermidine vibriobactin cannot be synthesized. While none of these mutants can produce vibriobactin, *vibF* and *nspC/nspCvibF* mutants have opposite biofilm phenotypes. One possible explanation for this observation is that in *ΔvibF*, norspermidine may be accumulating as it is not being converted into vibriobactin. To test this hypothesis, total polyamines were extracted from cells as well as the culture media and quantified using HPLC. HPLC data did not show any differences in norspermidine within the cell extracts from wild-type or *ΔvibF* planktonic or biofilm cells.

Since no differences in norspermidine levels were present in the cells I hypothesized that excess norspermidine was being exported out of the cells to maintain polyamine homeostasis. However, when media extracts were analyzed using liquid chromatography, no norspermidine was present in the culture media, indicating that norspermidine is not being exported out of the cell. Since no norspermidine differences were seen in the HPLC results I hypothesized that it was being modified and decided to try using conditioned media (CM) to see if wild-type biofilm formation would be affected.

In an effort to determine if the signal causing the increase in biofilm formation is an internal or external signal, conditioned media (CM) biofilm assays were utilized. I hypothesized that if the signal was present in the culture medium wild-type biofilm formation would increase with the addition of *AvibF* media. In order to confirm that this effect was possibly due to a modified form of norspermidine, wild-type and *ΔnspS* biofilm formation was quantified. The *ΔnspS* mutant is defective in the putative norspermidine sensor protein, NspS. The *ΔnspS* mutant cannot respond to exogenous norspermidine; therefore, if the signal is norspermidine this mutant will not show any response. Two other mutants were used to test this hypothesis, a mutant defective in norspermidine synthesis (*ΔnspC*), and a *nspC* overexpression mutant (*pnspC*). The *pnspC* mutant forms 3-5 fold more biofilms than wild-type; however, despite overexpressing the *nspC* gene, no increases in internal or external norspermidine are detectable in this strain (Parker *et al.*, 2012). This could possibly be explained by the hypothesis that in this mutant norspermidine is being modified and exported out of the cells and is increasing biofilm formation as an extracellular signal. These mutants were used with the expectations that *ΔnspC* would not have any effect on biofilm formation and that the *pnspC* would lead to an increase in wild-type biofilm formation.

Wild-type biofilm formation was decreased in all CM biofilms compared to fresh LB, with the exception of the overexpression mutant CM which showed comparable biofilm growth. Wild-type CM and $\Delta nspC$ CM supported comparable biofilm growth for wild-type, with about half the growth produced in LB. $\Delta vibF$ CM caused a significant increase in biofilm formation for wild-type compared to both wild-type and $\Delta nspC$ CM. Wild-type biofilm formation when grown in $nspC$ overexpression CM was the most comparable to the growth in fresh LB alone. With the exception of the $nspC$ overexpression CM all other CMs tested had a significant reduction in wild-type biofilm formation when compared to LB alone. $\Delta nspS$ did not show any change in biofilm growth for any media condition tested (Fig. 22). Planktonic cell growth was comparable for both wild-type and $\Delta nspS$ for all media conditions tested (Fig. 23).

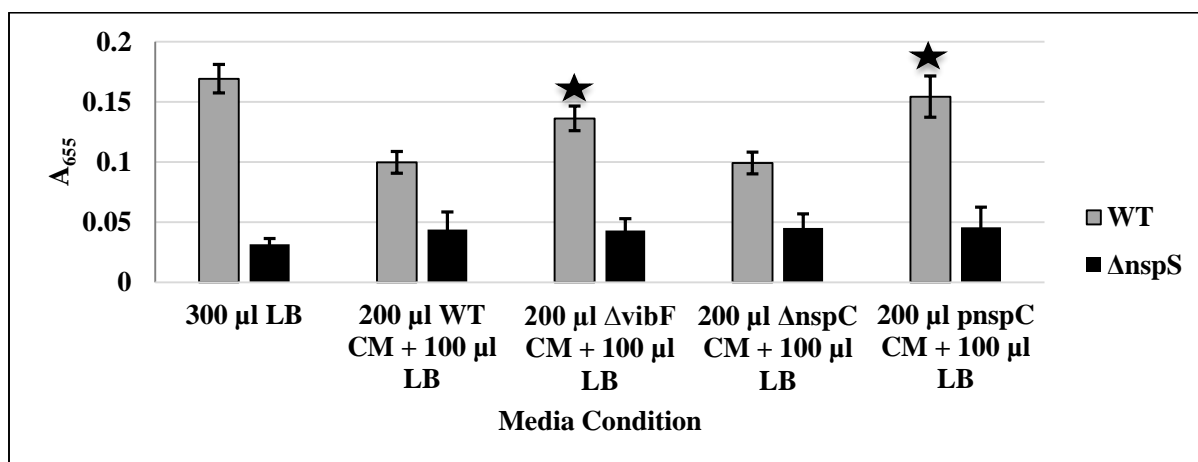


Fig. 22: Assessing the effect of conditioned medium on wild-type and $\Delta nspS$ biofilm formation after 24 hours. Both strains were grown in one of five media conditions and biofilm formation was quantified at 24 hours. Conditioned mediums were prepared from log phase cultures as described previously. As a control both strains were grown in fresh LB and for experimental conditions they were grown in either 200 μ l wild-type (WT) CM with 100 μ l fresh LB, 200 μ l $\Delta vibF$ CM with 100 μ l fresh LB, 200 μ l $\Delta nspC$ CM with 100 μ l fresh LB, or 200 μ l $pnspC$ CM with 100 μ l fresh LB. A star represents a statistically significant difference between wild-type biofilm growth in that mutant conditioned media compared to wild-type conditioned media. A p-value <0.05 was considered significant. Data represents the average of four biological replicates for each condition, error bars represent standard deviation.

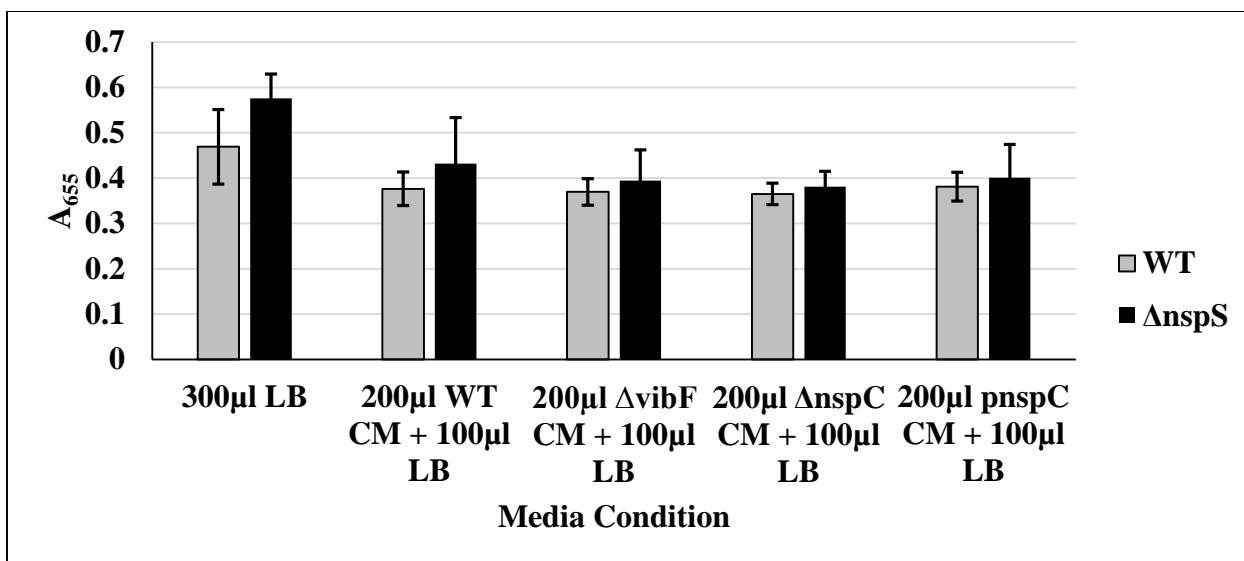


Fig. 23: Planktonic growth for wild-type and *ΔnspS* in response to conditioned medium. Both strains were grown in one of five media conditions and planktonic cell growth was quantified at 24 hours. Conditioned mediums were prepared from log phase cultures as described previously. As a control both strains were grown in fresh LB and for experimental conditions they were grown in either 200 μl wild-type (WT) CM with 100 μl fresh LB, 200 μl *ΔvibF* CM with 100 μl fresh LB, 200 μl *ΔnspC* CM with 100 μl fresh LB, or 200 μl *pnsnC* CM with 100 μl fresh LB. Data represents the average of four biological replicates for each condition, error bars represent standard deviation.

Effect of iron levels and siderophore synthesis on gene expression

Biofilms assays showed that conditioned media from *ΔvibF* generates an increase in wild-type biofilm formation, demonstrating that a secreted signal might be causing the increased biofilm growth. To gain insight into the nature of this signal and other effects of iron on biofilms, I decided to investigate the effect of iron levels and siderophore synthesis on gene transcript levels. I had hoped to use *vps* promoter fusion assays to determine if the *vps* genes were being upregulated in response to this signal. However, *vps* assays did not generate any clear results in regards to whether or not the *vps* genes were being upregulated. Therefore, I decided to use qPCR as a more sensitive assay to determine if VPS synthesis genes (*vpsL* and *vpsA*) were being differentially regulated in the *ΔvibF* mutant and in response to iron in planktonic and biofilm cells. To further characterize this system we also

looked at the transcript levels of *nspC*, *vibF*, and *speG* genes. The *speG* gene encodes a spermidine *N*-acetyltransferase, which can presumably acetylate norspermidine as well (Filippova *et al.*, 2015).

One strategy cells use to maintain polyamine homeostasis and avoid polyamine toxicity is through acetylating polyamines and transporting them out of the cell. Changes in expression levels of this gene could potentially help determine if acetylation could be possibly masking norspermidine in our HPLC analysis and making it undetectable via our HPLC assay. The RNA polymerase β -subunit gene *rpoB* was used as an internal control for all samples. I hypothesized that several trends in transcription would be present; first I expected to see upregulation in *vps* genes in the biofilm samples compared to planktonic and second I expected to see an increase in *vibF* transcription under iron-deplete conditions. Furthermore, I hypothesized that I would see an increase in *nspC* transcription under iron-deplete conditions and that this would likely coincide with increased *speG* transcription to possibly mitigate polyamine toxicity. In wild-type iron-replete biofilm cells, *vpsL* and *vpsA* transcript levels were increased 1.97 and 3.52 fold respectively; under iron-deplete conditions the same trend was seen with *vpsL* and *vpsA* transcript levels increasing 1.96 and 2.42 fold respectively. The increased levels of both *vps* gene transcripts is consistent in wild-type with *vpsA* showing higher transcript levels regardless of iron availability. In Δ *vibF* biofilms, both of the *vps* gene transcript levels were increased regardless of iron availability, but in Δ *vibF*, *vpsL* transcript levels were higher than *vpsA* transcripts.

Unfortunately, no clear trend was present in *vibF* transcript levels for wild-type in iron-replete conditions. In wild-type grown under iron-deplete conditions, *vibF* transcript levels were decreased 0.18 fold in biofilm cells. In Δ *vibF*, *vibF* transcript levels were

increased 2 fold in biofilm cells regardless of iron availability. *nspC* transcript levels were decreased 0.35-0.66 fold in all biofilm samples compared to the respective planktonic cells regardless of iron availability. In wild-type biofilm cells *speG* transcript levels were decreased 0.62 fold compared to planktonic cells, but *speG* transcript levels were variable in $\Delta vibF$ and no clear trend was observable (Fig. 24).

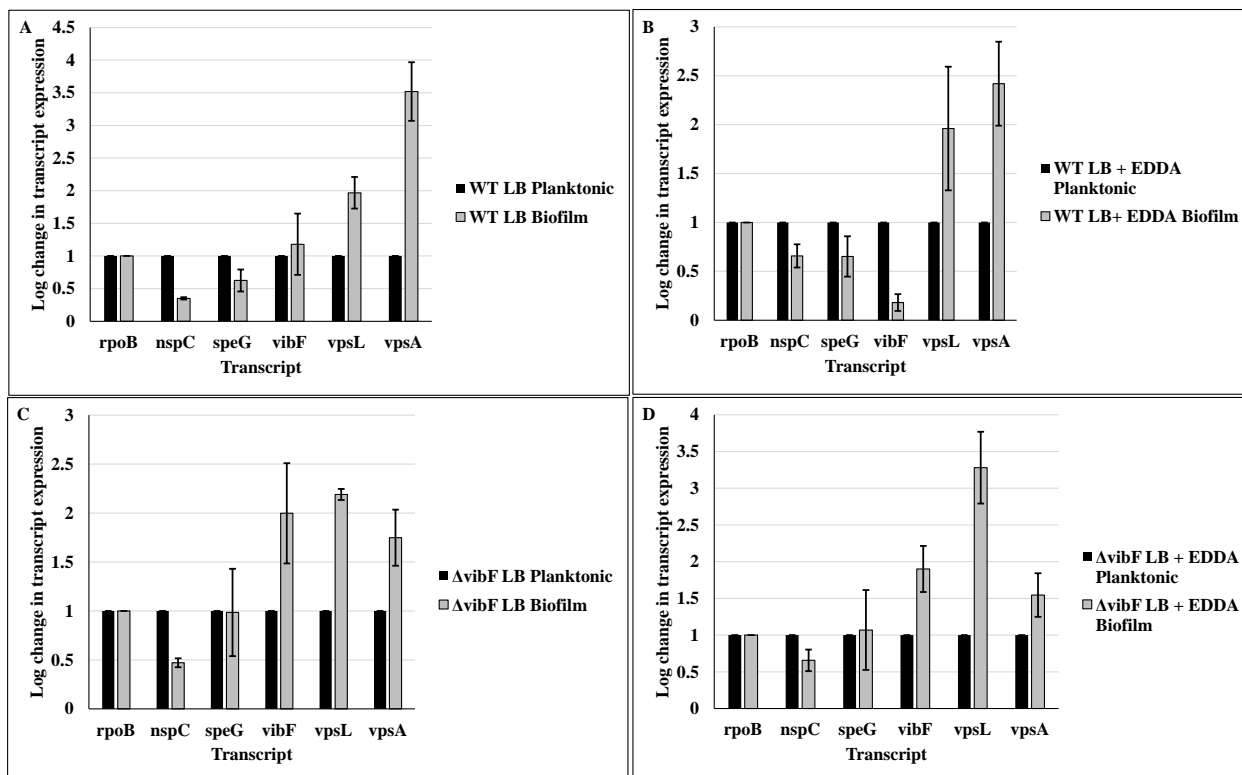


Fig. 24: Transcript levels in wild-type and $\Delta vibF$ planktonic and biofilm cells.

Transcript levels were quantified for *nspC*, *speG*, *vibF*, *vpsL*, and *vpsA* from biofilm and the associated planktonic cells using qPCR for wild-type cells grown in iron-replete conditions (A), wild-type cells grown in iron-deplete conditions (B) and $\Delta vibF$ grown in iron-replete conditions (C) and iron-deplete conditions (D). Data represents two biological replicates and error bars represent standard error and are included to show both consistency and variability across the two replicates. Each biological replicate consists of five technical replicates. Statistical significance between samples was not calculated due to small sample size.

Next, I wanted to investigate what differences in gene regulation were present between planktonic cells or biofilm cells in response to iron availability. I hypothesized that several trends in transcription would be present; under iron-deplete conditions *vibF*, *nspC*,

and *speG* would be upregulated in order to synthesize vibriobactin for iron uptake, norspermidine for vibriobactin synthesis, and possibly SpeG to maintain norspermidine homeostasis. In wild-type and $\Delta vibF$ planktonic cells no difference in transcript levels were observed between iron-replete and iron-deplete conditions for *nspC*, *vpsL*, and *vpsA*. *vibF* transcript levels were increased 6.48 fold and *speG* transcript levels were increased 2.66 fold in wild-type iron-deplete planktonic cells compared to wild-type iron-replete planktonic cells. In $\Delta vibF$, *vibF* and *speG* transcript levels were increased 2.48 and 2.71 fold respectively, under iron-deplete conditions in planktonic cells. In $\Delta vibF$ planktonic cells under iron-deplete conditions, *nspC* transcript levels were increased 1.13 fold, *vpsL* transcript levels were decreased 0.58 fold, and *vpsA* transcript levels were decreased 0.81 fold. I hypothesized that *vps* transcript levels would decrease in biofilms grown under iron-deplete conditions, since biofilm growth is decreased under these conditions. Surprisingly, in wild-type iron-deplete biofilms *vpsL* and *vpsA* transcript levels were increased 1.62 and 1.25 fold respectively and *vibF* transcript levels were decreased 0.79 fold compared to iron-replete conditions. Both *nspC* and *speG* transcript levels were increased in wild-type biofilms under iron-deplete conditions 1.34 and 2.24 fold respectively. In $\Delta vibF$ iron-deplete biofilms both *vpsL* and *vpsA* transcript levels were decreased 0.88 and 0.73 fold, *nspC* transcript levels were increased 1.44 fold, *speG* transcript levels were increased 3.24 fold, and *vibF* transcript levels were increased 1.89 fold compared to iron-replete conditions. *nspC* does not appear to be under iron regulation in wild-type or $\Delta vibF$ planktonic cells as transcript levels were comparable regardless of iron availability (Fig. 25).

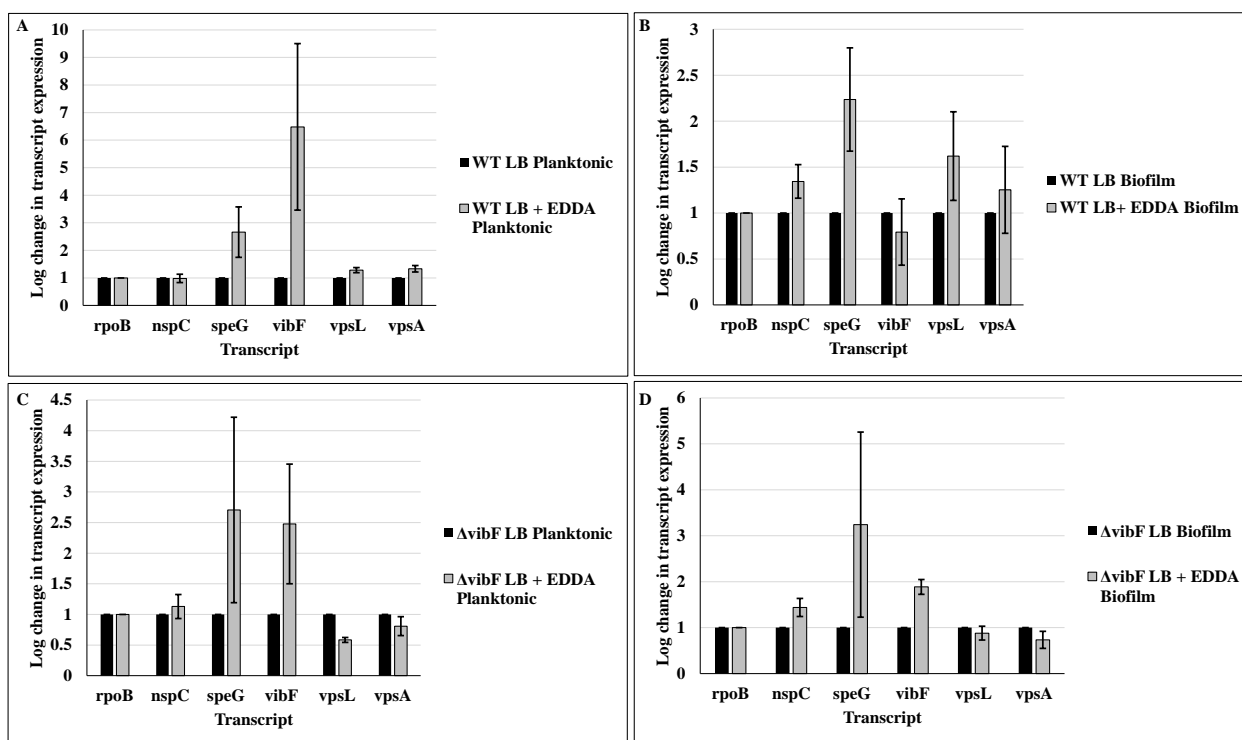


Fig. 25: Transcript levels between cells in either iron-replete or iron-deplete conditions. Transcript levels were quantified for *nspC*, *speG*, *vibF*, *vpsL*, and *vpsA* from biofilm and the associated planktonic cells using qPCR for wild-type planktonic cells grown in iron-replete and iron-deplete conditions (A), wild-type biofilm cells grown in iron replete and iron-deplete conditions (B), *AvibF* planktonic cells grown in iron-replete and iron-deplete conditions (C) *AvibF* biofilm cells grown in iron-replete and iron-deplete (D). Data represents two biological replicates and error bars represent standard error and are included to show both consistency and variability across the two replicates. Each biological replicate represents five technical replicates. Statistical significance between samples was not calculated due to small sample size.

Comparing biofilm and planktonic cells grown in the same iron conditions and between iron-replete and iron-deplete conditions showed some clear trends in regards to biofilm associated genes being upregulated in biofilm cells compared to planktonic cells. But, these comparisons do not really show any clear trend in regards to the hypothesis that norspermidine is the signal that is generating the increase in biofilm formation, specifically *nspC* is decreased in biofilm cells compared to planktonic cells and while this trend is clear, no clear trend is present in *speG* or *vibF* transcription levels.

The next step was to look at trends in transcript levels with in either wild-type or *ΔvibF* and compare each against planktonic cells grown in iron-replete conditions. In both wild-type iron-replete and iron-deplete biofilms, *nspC* transcript levels were decreased 0.35 and 0.62 fold respectively, compared to iron-replete planktonic cells. In wild-type iron-replete biofilm cells *vpsL* transcript levels were increased 1.97 fold, *vpsA* transcript levels were increased 3.52 fold, *speG* transcript levels were decreased 0.63 fold, and *vibF* transcript levels were increased 1.17 fold compared to wild-type iron-replete planktonic cells. In wild-type iron-deplete biofilm cells *nspC*, *vpsL*, and *vpsA* are comparable to wild-type iron-replete transcript levels. As these cells are starved for iron it would be expected that vibriobactin is being synthesized and in these cells *vibF* transcript levels were increased 6.48 fold, suggesting that vibriobactin is being produced; under iron-deplete conditions *speG* transcript levels were increased 2.66 fold in planktonic cells. In wild-type iron-deplete biofilms *speG* transcription is comparable to wild-type iron-replete planktonic cells, *vpsL* and *vpsA* transcript levels were increased 3.52 and 3.16 fold in iron-deplete biofilm cells (Fig.26). In *ΔvibF*, *nspC* transcript levels were decreased 0.47 fold in iron-replete biofilms and 0.66 fold in iron-deplete biofilms, consistent with the decrease in transcript levels seen in wild-type biofilms. Both *vpsL* and *vpsA* transcript levels were increased 2.19 and 1.74 fold respectively, in iron-replete *ΔvibF* biofilms.

No change was seen in *speG* transcription compared to *ΔvibF* iron-replete planktonic cells, but *vibF* transcript levels were increased 2 fold. In *ΔvibF* iron-deplete planktonic cells *speG* transcript levels were increased 2.71 fold and *vibF* transcript levels were increased 2.48 fold compared to *ΔvibF* iron-replete planktonic cells. Both *vps* gene transcript levels were decreased in *ΔvibF* iron-deplete planktonic cells compared to iron-replete planktonic cells.

In $\Delta vibF$ iron-deplete biofilm cells *speG* transcript levels were increased 1.41 fold, *vibF* transcript levels were increased 3.97 fold, *vpsL* transcript levels were increased 1.93 fold, and *vpsA* transcript levels were increased 1.18 fold compared to $\Delta vibF$ iron-replete planktonic cells (Fig. 27).

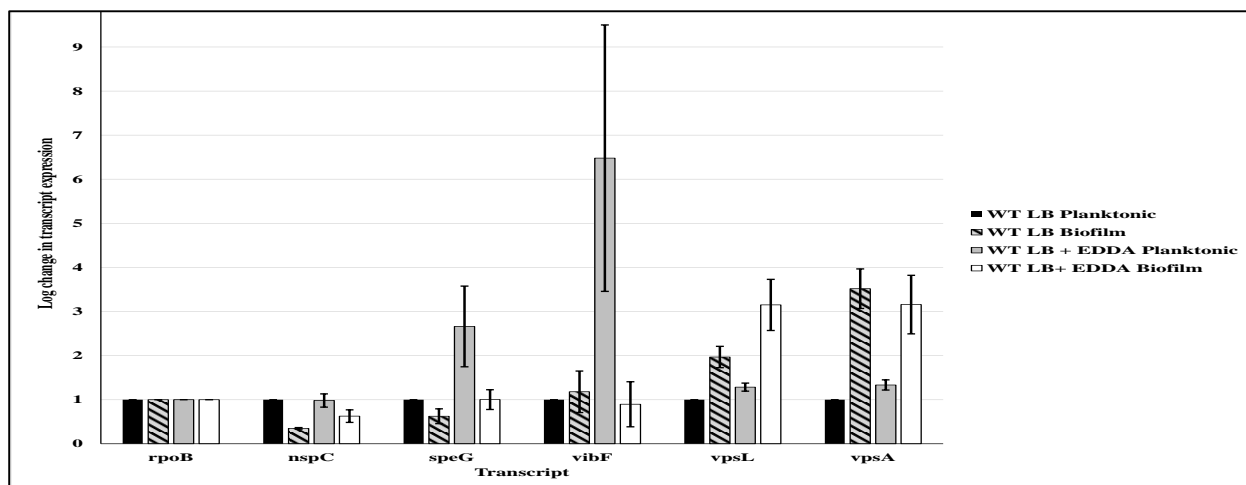


Fig. 26: Transcript levels in wild-type biofilm and planktonic cells compared against wild-type iron-replete transcript levels. Data represents two biological replicates and error bars represent standard error and are included to show both consistency and variability across the two replicates. Statistical significance between samples was not calculated due to small sample size.

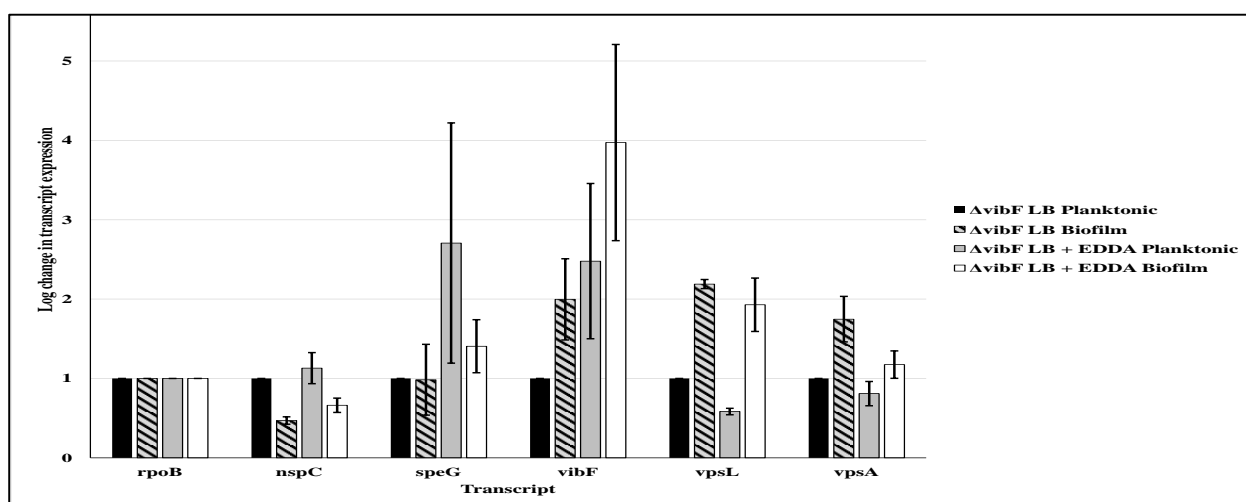


Fig. 27: Transcript levels in $\Delta vibF$ planktonic and biofilm cells compared against $\Delta vibF$ iron-replete planktonic cells. Data represents two biological replicates and error bars represent standard error and are included to show both consistency and variability across the two replicates. Statistical significance between samples was not calculated due to small sample size.

The final question was to determine what differences were present in transcript levels between $\Delta vibF$ and wild-type planktonic or biofilm cells. I hypothesized that some modified form of norspermidine is accumulating either in the cell or outside the cell in $\Delta vibF$ and is responsible for the increased biofilm growth. *nspC* and *speG* transcript levels were increased in both $\Delta vibF$ planktonic and biofilm cells compared to wild-type planktonic and biofilms, regardless of iron availability. *vibF* transcript levels were increased in all $\Delta vibF$ samples with the exception of when comparing $\Delta vibF$ biofilm against wild-type biofilm under iron-replete conditions. *vps* transcript levels were decreased in all $\Delta vibF$ samples with the exception of $\Delta vibF$ iron-deplete planktonic cells against wild-type iron-deplete planktonic cells (Fig. 28).

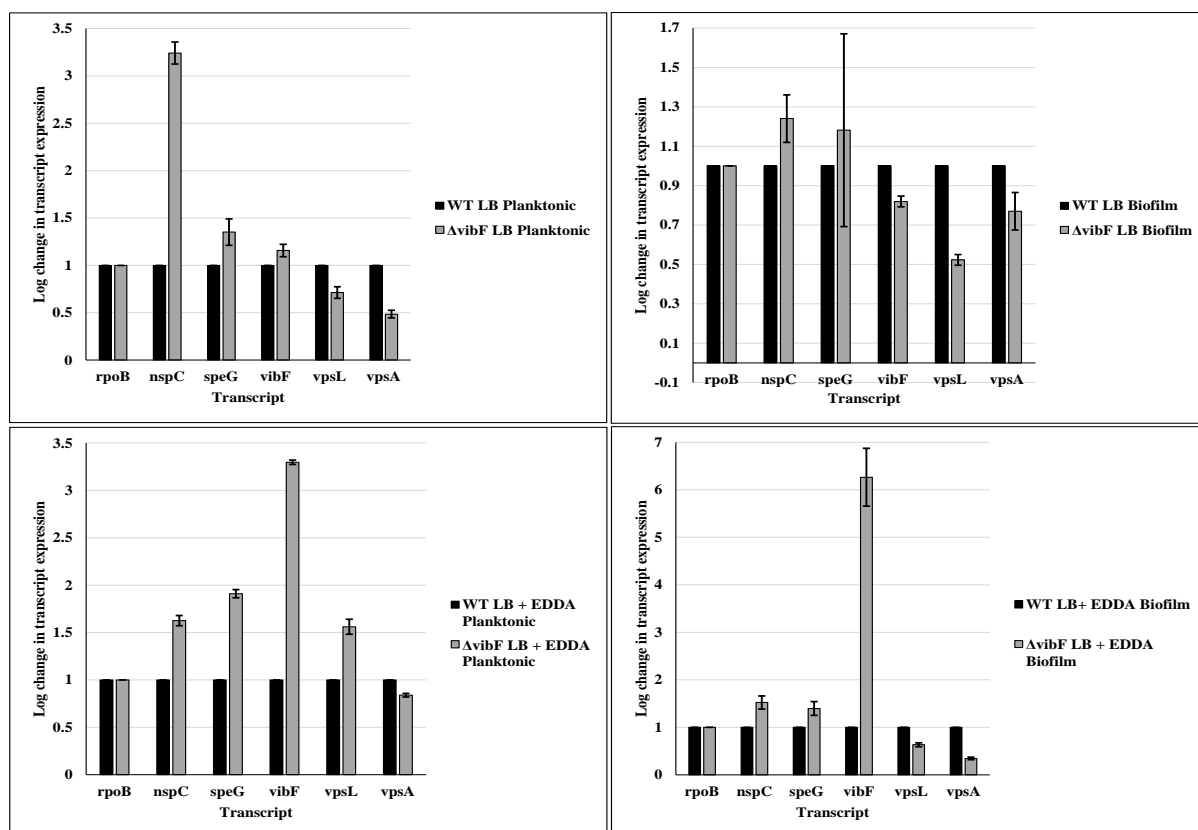


Fig. 28: Transcript levels in $\Delta vibF$ planktonic and biofilm cells compared against wild-type planktonic and biofilm cells under the same iron conditions. Data represents a single biological replicate of two technical replicates and error bars represent standard error and are included to show both consistency and variability across the two replicates.

Discussion

The purpose of this study was to investigate a potential link between iron availability, norspermidine synthesis, and biofilm formation. Through this work I have shown that iron availability and inhibition of vibriobactin synthesis have opposite effects on biofilm formation. In iron-deplete media biofilm formation was significantly inhibited in *V. cholerae* O139 and this decrease was similar to the decrease reported in a different serogroup of this bacterium, *V. cholerae* O1 El Tor (Mey *et al.*, 2005a). In contrast, inhibition of vibriobactin synthesis generated a significant increase in biofilm formation. My data suggest that this increased biofilm phenotype is a secondary effect rather than an effect related to iron levels, as the increase is seen regardless of iron availability. Inhibiting vibriobactin synthesis not only increased biofilm formation, but also changed biofilm morphology, where this mutant formed a lawn like biofilm rather than the mushroom-like macrocolonies observed in the wild-type. In addition, this work has demonstrated that the increase in biofilm formation can be nullified through inhibiting norspermidine synthesis in the vibriobactin mutant, suggesting that norspermidine could be responsible for the increased biofilm formation. In further support of norspermidine or another self-produced signal playing a role in the increased biofilm formation, I have shown that conditioned media from the vibriobactin mutant leads to an increase in wild-type biofilm formation compared to wild-type conditioned media. Quantification of gene expression using real-time PCR showed that both *vpsA* and *vpsL* genes were upregulated in biofilms. In addition, transcription of *nspC* was downregulated in biofilm samples, a surprising result given that norspermidine is required for normal levels of

biofilm formation. One explanation for this observation may be that norspermidine could be accumulating in the biofilm environment, as biofilms are characterized by high cell density and low rates of diffusion.

In an effort to quantify levels of iron in and outside of the cells under the conditions of my experiments to confirm that the cells were being starved of iron, we used ICP. I expected three trends to be abundantly clear from this analysis: first, spent media samples with EDDA should have higher iron concentrations because cells grown in these conditions should have impaired iron uptake. Second, fresh media should have identical iron concentrations regardless of the presence of EDDA. Prior to being added to the media, EDDA is deferrated, meaning that it is freed of any bound iron leaving only EDDA in the precipitate (Rogers, 1973). Third, lower levels of iron in cells grown in the EDDA media and even lower levels in vibriobactin synthesis mutant. Unfortunately this experiment did not generate any clear data as to whether or not the cells were being starved of iron. For all samples tested with the exception of the vibriobactin uptake mutant, there was no significant difference in iron levels within the cells or within the media these strains were grown in. Due to lack of time and resources this experiment was only performed once, therefore, I cannot be confident in the accuracy of the results. One possible explanation for the variation in total iron across the cell extracts and media could be due to the small sample volumes. Each sample had a total volume of two milliliters and was divided into the cellular and media portions, this volume is well below the volume that is typically used for ICP and could explain the lack of any clear trend.

Because I was not able to demonstrate using ICP analysis that the conditions I was using led to iron starvation in the cells, I decided to measure *vibF* transcript levels under my

experimental conditions. *vibF* transcript levels could be quantified using qPCR because the primers used amplify a region of *vibF* that is outside of the internal deletion, so while the gene is being transcribed to mRNA, it is not being translated into a functional protein. Real-time PCR data showed that transcription of the *vibF* gene was increased under iron-deplete conditions in wild-type planktonic cells, demonstrating that these cells are activating the vibriobactin pathway to acquire iron. In addition, *vibF* was upregulated under iron-replete conditions in biofilms formed by the $\Delta vibF$ mutant; and in both planktonic and biofilm cells under iron-deplete conditions, indicating that *vibF* mutants are more starved of iron as expected. These results indicate that both EDDA treatment and deletion of the *vibF* gene leads to iron starvation.

For all strains tested, wild-type, $\Delta vibF$, *viuA::tet^r*, $\Delta vibF\Delta nspC$, and $\Delta nspC$, biofilm growth was repressed in iron-deplete media compared to biofilm growth under iron-replete conditions. My results support previous work, which showed *V. cholerae* biofilm growth was decreased with the addition of EDDA in a concentration dependent manner, supporting a role for iron in normal biofilm growth and supporting the hypothesis that iron-deficiency would decrease biofilm formation (Mey *et al.*, 2005a). Next, I hypothesized that $\Delta vibF$ and *viuA::tet^r* biofilm growth would be inhibited when compared to wild-type and that this decrease would be exacerbated by iron-depletion as both of these strains are inhibited in vibriobactin-mediated iron uptake. Surprisingly, biofilm growth for *viuA::tet^r* very closely mimicked wild-type growth regardless of iron availability, and $\Delta vibF$ formed significantly increased biofilms regardless of iron availability, suggesting that this increased biofilm formation is due to a secondary effect and not necessarily in response to iron availability. Next, we investigated if biofilm morphology was altered in $\Delta vibF$ using SEM. Wild-type

formed distinct macrocolonies with the characteristic well-ordered mushroom like structure, regardless of iron availability, and $\Delta vibF$ formed a more sheet-like biofilm. No mushroom like structures were visible in $\Delta vibF$ when viewed at the same magnification, suggesting that this secondary effect of inhibited vibriobactin synthesis plays some role in the ordering of the biofilm matrix, or at least the formation of macrocolonies.

Based on these results I had to reject my original hypothesis and propose a new hypothesis, where deletion of *vibF* leads to the accumulation of a vibriobactin precursor and that this precursor is a pro-biofilm signal. Specifically, I hypothesized that this signal was norspermidine due to three observations: first, norspermidine, which forms the backbone of vibriobactin, is not directed into vibriobactin synthesis in the $\Delta vibF$ mutant and could be accumulating, second, addition of norspermidine to a growth culture significantly increases biofilm formation, and third, inhibition of norspermidine synthesis leads to a large reduction of biofilm formation (Wyckoff *et al.*, 2001; Karatan *et al.*, 2005; Lee *et al.*, 2009). When $\Delta vibF$ was compared with a $\Delta vibF/\Delta nspC$ double mutant the increased biofilm formation was completely abolished and instead the $\Delta vibF/\Delta nspC$ double mutant shows a significant decrease in biofilm formation when compared to the wild-type. The decrease in biofilm formation was even further exacerbated in the iron-deplete conditions for the double mutant. The decrease in biofilm formation observed in the $\Delta vibF/\Delta nspC$ double mutant was also seen in a $\Delta nspC$ mutant, suggesting that in regards to biofilm formation *nspC* is epistatic over *vibF*. While these data suggest that the increased biofilm formation in $\Delta vibF$ could be due to increases in norspermidine through an effort to produce vibriobactin it is not conclusive. In an effort to test whether norspermidine is accumulating and is the signal behind the increased

biofilm phenotype, total polyamines were extracted from biofilm cells, planktonic cells, and the culture media and analyzed via liquid chromatography.

Preliminary HPLC data did not show any increase in norspermidine levels in *ΔvibF* planktonic or biofilm cell extracts when compared against the wild-type. While this does not prove that norspermidine is the signal leading to increased biofilm formation in *ΔvibF*, it does not necessarily disprove the norspermidine hypothesis. Mutants overexpressing *nspC* from a plasmid have been shown to form 3-5 fold more biofilm than the wild-type (Parker *et al.*, 2012). However, even under these conditions, internal norspermidine levels do not show any increase. Norspermidine can be toxic to cells if internal concentrations are too high, in response to high intracellular concentrations, cells could secrete norspermidine into the extracellular environment in an effort to avoid norspermidine toxicity. However, no norspermidine was present in the media; therefore it does not seem to be secreted as is, consistent with previous work from our lab (Parker *et al.*, 2012). Sometimes polyamines are modified by acetylating the primary amine groups prior to secretion in order to facilitate transport across the cell membrane. One such strategy involves the use of the enzyme spermidine *N*-acetyltransferase, SpeG, which is encoded by the *speG* gene. In *E. coli*, SpeG has been shown to be involved in mitigating spermidine toxicity stress. SpeG catalyzes the transfer of an acetyl group from acetyl coenzyme A (AcCoA) to the primary amine group of spermidine, neutralizing the molecules charge and leading to its transport out of the cell (Filippova *et al.*, 2015). In *V. cholerae* SpeG has recently been shown to acetylate both spermidine and spermine. The study did not test norspermidine for unknown reasons but based on the similarity in structure between spermidine and norspermidine, which differ in only a single methylene group, it is reasonable to speculate that SpeG could acetylate

norspermidine (Filippova *et al.*, 2015). If norspermidine is accumulating in the cell, it is possible that the cells would experience norspermidine toxicity, unless SpeG acts to acetylate norspermidine leading to its transport. If norspermidine is being acetylated this could possibly explain why it was not detected in HPLC analysis of wild-type and $\Delta vibF$ conditioned media. In order to detect polyamines via HPLC followed by UV-Vis spectroscopy, we benzoylate them, which leads to the addition of a benzoyl group to the amine groups. If norspermidine is being acetylated at the primary amine groups, this could be preventing benzoylation of the polyamine at these positions. While the secondary amine group should still be benzoylated, the polarity of the compound would be changed. This in turn would also change its mobility in liquid chromatography, which explains why it may not have been detected using current protocols. New protocols will have to be developed in order to detect this molecule.

An alternative strategy to determine if norspermidine is the signal causing the increased biofilm formation used conditioned media (CM) biofilm assays. I hypothesized that norspermidine was being acetylated and transported out of the cells and that acetylated norspermidine was the pro-biofilm signal. To test this hypothesis, I reasoned that CM from $\Delta vibF$ would lead to an increase in wild-type biofilm formation compared to CM from a wild-type culture. In addition to $\Delta vibF$ CM I also tested $\Delta nspC$ CM and $p nspC$ (wild-type cells expressing $nspC$ from a plasmid) CM. If norspermidine in some form is in fact the pro-biofilm signal in this system, then $\Delta nspC$ CM should not have any effect on wild-type biofilm growth, whereas CM from the $p nspC$ strain should lead to an increase in wild-type biofilm formation. As a control for all conditioned media tested, we also tested their effect on a $\Delta nspS$ mutant. As described previously, our lab has shown that norspermidine leads to

an upregulation of biofilm formation through the NspS/MbaA pathway. I reasoned that in addition to norspermidine, a modified version of norspermidine could also act through this pathway to affect biofilms. If this is the case, *AnspS* should not respond to CM from any of the strains. All CM tested, with the exception of *pnsnC*, showed decreased biofilm formation in comparison to fresh LB. The decreased biofilm growth is most likely due to lack of nutrients in the CM as these cultures were grown to log phase and would most likely deplete the media of nutrients. Wild-type biofilm growth was nearly identical for both wild-type CM and *AnspC* CM, but was increased when grown in *AvibF* CM. The fact that both *AvibF* CM and *pnsnC* CM generated increased wild-type biofilm growth supports the hypothesis that some form of norspermidine is responsible for the increased biofilm phenotype. *AnspS* did not show any response to wild-type, *AvibF*, *AnspC*, or *pnsnC* CM, further supporting the hypothesis that a modified form of norspermidine may be the pro-biofilm signal.

The next approach to elucidate the details of this system involved looking at transcript levels of various genes in wild-type and *AvibF* biofilm and planktonic cells in response to iron availability to see if any clear trends in transcription were present. In order to assess the accuracy of the real-time data, I wanted to show that when comparing biofilm cells against planktonic cells that the biofilm matrix genes, *vpsL* and *vpsA*, would have increased transcript levels. Real-time PCR data shows that both *vps* gene transcript levels were increased in biofilms compared to planktonic cells, which suggests that this data can be trusted. I hypothesized that *vps* gene transcription would mirror the biofilm assay results, with *AvibF* biofilm showing the highest level of *vps* transcription out of all samples; furthermore I expected to see decreases in *vps* transcription in iron-deplete biofilms compared to iron-replete biofilms for both wild-type and *AvibF*. My results do not show

these trends; instead *vps* transcription is slightly decreased in $\Delta vibF$ biofilm compared to wild-type biofilm. It is possible that the increased biofilm growth could be due to post-transcription effects such as increased translation of proteins encoded by the *vps* genes or post-transcriptional modification of any of these proteins leading to higher enzymatic activity. Alternatively, the increased biofilm could be due to increased protein or extracellular DNA components of the matrix rather than the exopolysaccharides.

As mentioned above, I hypothesized that the increase in $\Delta vibF$ biofilm formation is caused by a modified form of norspermidine, as liquid chromatography did not show any increases in norspermidine in or outside the cells. In order to determine if norspermidine is being acetylated and transported out of the cell, I decided to investigate *nspC* and *speG* transcript levels to try and answer this question. I hypothesized that *nspC* transcript levels would be increased in $\Delta vibF$ in order to supply norspermidine for vibriobactin synthesis and that because of this increased production of norspermidine, *speG* transcript levels would also be increased to help deal with polyamine toxicity and maintain polyamine homeostasis. Real-time PCR analysis shows that both *nspC* and *speG* transcript levels were increased in $\Delta vibF$ biofilm and planktonic cells compared to wild-type regardless of iron availability. These data suggest, that norspermidine is being produced at higher levels in $\Delta vibF$ compared to wild-type and that $\Delta vibF$ cells may be producing more SpeG to maintain polyamine homeostasis by acetylating norspermidine prior to transport out of the cell. I also found that in all biofilm samples *nspC* transcript levels were reduced compared to planktonic cells, showing that norspermidine synthesis has been downregulated in these cells. I hypothesize that modified levels of norspermidine are accumulating within the biofilm environment due to the conditions within the biofilm. Biofilms are characterized by high cell density

contained within the biofilm matrix, this high cell density and the biofilm matrix limit the rate of diffusion for molecules within the biofilm environment. The lower rates of diffusion and the high cell density could be leading to significant increases in modified norspermidine within the biofilm environment and this high concentration of norspermidine could be signaling to the cells that norspermidine levels are approaching toxic levels and need to stop producing norspermidine. Based on the real-time PCR results, *nspC* does not appear to be under regulation by iron, as transcript levels are not decreased under iron-deplete conditions. In order to determine if *nspC* was under Fur regulation, I analyzed the 200 bp region upstream of the *nspC* start site using published *V. cholerae* Fur consensus sequences (Mey *et al.*, 2005b). Multiple sequence alignments and pair wise analyses did not find any potential Fur consensus sequence in the *nspC* upstream region, showing that *nspC* is not under iron regulation through Fur (data not shown).

In conclusion, iron deficiency and inhibition of vibriobactin synthesis have opposite effects on biofilm formation. Iron starvation through addition of EDDA to the culture media significantly inhibits biofilm morphology through an unknown pathway. Inhibition of vibriobactin synthesis significantly increases biofilm formation. We hypothesize that this increase is due to accumulation of modified, possibly acetylated, norspermidine. Future work will have to be directed at this pathway to understand how these cells regulate norspermidine synthesis and how norspermidine toxicity is mitigated. To conclusively identify the pro-biofilm signal as a modified form of norspermidine or any other molecule, metabolomics and media fractionation experiments will need to be completed.

References

- Bomchil, N., Watnick P., and Kolter R., (2003) Identification and characterization of a *Vibrio cholerae* gene, *mbaA*, involved in maintenance of biofilm architecture. *J of Bacteriol* **185**: 1384-1390.
- Butterton, J.R., Choi M.H., Watnick P.I., Carroll P.A., and Calderwood S.B. (2000) *Vibrio cholerae* VibF is required for vibriobactin synthesis and is a member of the family of nonribosomal peptide synthetases. *J of Bacteriol* **182**: 1731-1738.
- Butterton, J.R., Stoebner J.A., Payne S.M., and Calderwood S.B. (1992) Cloning, sequencing, and transcriptional regulation of *viuA*, the gene encoding the ferric vibriobactin receptor of *Vibrio cholerae*. *J of Bacteriol* **174**: 3729-3738.
- Cockerell, S.R., Rutkovsky A.C., Zayner J.P., Cooper R.E., Porter L.R., Pendergraft S.S., Parker Z.M, McGinnis M.W., and Karatan E. (2014) *Vibrio cholerae* NspS, a homologue of ABC-type periplasmic solute binding proteins, facilitates transduction of polyamine signals independent of their transport. *Microbiology* **160**: 832-843.
- Crosa, J.H., and C.T. Walsh C.T. (2002) Genetics and assembly line enzymology of siderophore biosynthesis in bacteria. *Microbiol Mol Biol Rev* **66**: 223-249.
- Davis, B.M., Quinones M., Pratt J., Ding Y., and Waldor M.K. (2005) Characterization of the small untranslated RNA RyhB and its regulon in *Vibrio cholerae*. *J of Bacteriol* **187**: 4005-4014.
- Doherty, C.P. (2007) Host-pathogen interactions: the role of iron. *The J of Nutrition* **137**: 1341-1344.

- EPA, U. (2011) U. S. Method 6010C: Inductively coupled plasma-atomic emissions spectrometry.
- Filippova, E.V., Kuhn, M.L., Osipiuk, J., Kiryukhina, O., Joachimiak, A., Ballicora, M.A., and Anderson, W.F. (2015) A novel polyamine allosteric site of SpeG from *Vibrio cholerae* is revealed by its dodecameric structure. *J Mol Biol* **427**: 1316-1334.
- Fong, J.C., Syed, K.A., Klose, K.E., and Yildiz, F.H. (2010) Role of *Vibrio* polysaccharide (*vps*) genes in VPS production, biofilm formation and *Vibrio cholerae* pathogenesis. *Microbiology* **156**: 2757-2769.
- Griffiths, G.L., Sigel, S.P., Payne, S.M. and Neilands, J.B. (1984) Vibriobactin, a siderophore from *Vibrio cholerae*. *The J of Biol Chem* **259**: 383-385.
- Hamana, K. and Matsuzaki, S. (1982) Widespread occurrence of norspermidine and norspermine in eukaryotic algae. *J of Biochem* **91**: 1321-1328.
- Haugo, A.J. and Watnick, P.I. (2002) *Vibrio cholerae* CytR is a repressor of biofilm development. *Mol Microbiol* **45**: 471-483.
- Huq, A., Colwell, R.R., Rahman, R., Ali A., Chowdhury, M.A., Parveen, S., Sack, D.A., and Russek-Cohen, E. (1990) Detection of *Vibrio cholerae* O1 in the aquatic environment by fluorescent-monoclonal antibody and culture methods. *Appl Environ Microbiol* **56**: 2370-2373.
- Kamruzzaman, M., Udden, S.M., Cameron, D.E., Calderwood, S.B., Nair, G.B., Mekalanos, J.J., and Faruque, S.M. (2010) Quorum-regulated biofilms enhance the development of conditionally viable, environmental *Vibrio cholerae*. *Proceedings of the National Academy of Sciences of the United States of America* **107**: 1588-1593.

- Karatan, E., Duncan, T.R., and Watnick, P.I. (2005) NspS, a predicted polyamine sensor, mediates activation of *Vibrio cholerae* biofilm formation by norspermidine. *J Bacteriol* **187**: 7434-7443.
- Karatan, E. and Watnick, P. (2009) Signals, regulatory networks, and materials that build and break bacterial biofilms. *Microbiology and Molecular Biology Reviews : MMBR* **73**: 310-347.
- Lam, M.S., Litwin, C.M., Carroll, P.A., and Calderwood, S.B. (1994) *Vibrio cholerae fur* mutations associated with loss of repressor activity: implications for the structural-functional relationships of fur. *J of Bacteriol* **176**: 5108-5115.
- Lee, J., Sperandio, V., Frantz, D.E., Longgood, J., Camilli, A., Phillips, M.A., and Michael, A.J. (2009) An alternative polyamine biosynthetic pathway is widespread in bacteria and essential for biofilm formation in *Vibrio cholerae*. *J Biol Chem* **284**: 9899-9907.
- Litwin, C.M., Boyko, S.A., and Calderwood, S.B. (1992) Cloning, sequencing, and transcriptional regulation of the *Vibrio cholerae fur* gene. *J of Bacteriol* **174**: 1897-1903.
- Mandlik, A., Livny, J., Robins, W.P., Ritchie, J.M., Mekalanos, J.J., and Waldor, M.K. (2011) RNA-Seq-based monitoring of infection-linked changes in *Vibrio cholerae* gene expression. *Cell host and Microbe* **10**: 165-174.
- Marshall, C.G., Hillson, N.J., and Walsh, C.T. (2002) Catalytic mapping of the vibriobactin biosynthetic enzyme VibF. *Biochem* **41**: 244-250.
- McGinnis, M.W., Parker, Z.M., Walter, N.E., Rutkovsky, A.C., Cartaya-Marin, C., and Karatan, E. (2009) Spermidine regulates *Vibrio cholerae* biofilm formation via transport and signaling pathways. *FEMS Microbiology Letters* **299**: 166-174.

- Metcalf, W.W., Jiang, W., Daniels, L.L., Kim, S.K., A. Haldimann, A., and Wanner, B.L. (1996) Conditionally replicative and conjugative plasmids carrying *lacZ* alpha for cloning, mutagenesis, and allele replacement in bacteria. *Plasmid* **35**: 1-13.
- Mey, A.R., Craig, S.A., and Payne, S.M. (2005a) Characterization of *Vibrio cholerae* RyhB: the RyhB regulon and role of *ryhB* in biofilm formation. *Infect Immun* **73**: 5706-5719.
- Mey, A.R., Wyckoff, E.E., Hoover, L.A., Fisher, C.R., and Payne, S.M. (2008) *Vibrio cholerae* VciB promotes iron uptake via ferrous iron transporters. *J of Bacteriol* **190**: 5953-5962.
- Mey, A.R., Wyckoff, E.E., Kanukurthy, V., Fisher, C.R., and Payne, S.M. (2005b) Iron and *fur* regulation in *Vibrio cholerae* and the role of *fur* in virulence. *Infect Immun* **73**: 8167-8178.
- Miethke, M. and Marahiel, M.A. (2007) Siderophore-based iron acquisition and pathogen control. *Microbiol Mol Biol Rev* **71**: 413-451.
- Miller, V.L. and Mekalanos, J.J. (1988) A novel suicide vector and its use in construction of insertion mutations: osmoregulation of outer membrane proteins and virulence determinants in *Vibrio cholerae* requires *toxR*. *J of Bacteriol* **170**: 2575-2583.
- Morgan, D.M. (1998) *Polyamine protocols*. Springer Science and Business Media.
- Occhino, D.A., Wyckoff, E.E., Henderson, D.P., Wrona, T.J., and Payne, S.M. (1998) *Vibrio cholerae* iron transport: haem transport genes are linked to one of two sets of *tonB*, *exbB*, *exbD* genes. *Mol Microbiol* **29**: 1493-1507.
- Olczak, T., Simpson, W., Liu, X., and Genco, C.A. (2005) Iron and heme utilization in *Porphyromonas gingivalis*. *FEMS Microbiol Rev* **29**: 119-144.

- Parker Siburt, C.J., Mietzner, T.A., and Crumbliss, A.L. (2012) FbpA--a bacterial transferrin with more to offer. *Biochimica et biophysica acta* **1820**: 379-392.
- Parker, Z.M., Pendergraft, S.S., Sobieraj, J., McGinnis, M.M., and Karatan, E. (2012) Elevated levels of the norspermidine synthesis enzyme NspC enhance *Vibrio cholerae* biofilm formation without affecting intracellular norspermidine concentrations. *FEMS Microbiol Lett* **329**: 18-27.
- Patel, C.N., Wortham, B.W., Lines, J.L., Fetherston, J.D., Perry, R.D., and Oliveira, M.A. (2006) Polyamines are essential for the formation of plague biofilm. *J of Bacteriol* **188**: 2355-2363.
- Rogers, H.J. (1973) Iron-Binding Catechols and Virulence in *Escherichia coli*. *Infect Immun* **7**: 445-456.
- Romling, U. and Amikam, D. (2006) Cyclic di-GMP as a second messenger. *Current opinion in microbiology* **9**: 218-228.
- Seliger, S.S., Mey, A.R., Valle, A.M., and Payne, S.M. (2001) The two TonB systems of *Vibrio cholerae*: redundant and specific functions. *Mol Microbiol* **39**: 801-812.
- Smith, J.L. (2004) The physiological role of ferritin-like compounds in bacteria. *Critical Reviews in Microbiology* **30**: 173-185.
- Stanley, N.R. and Lazazzera, B.A. (2004) Environmental signals and regulatory pathways that influence biofilm formation. *Mol Microbiol* **52**: 917-924.
- Tabor, C.W. and Tabor, H. (1985) Polyamines in microorganisms. *Microbiological Reviews* **49**: 81-99.
- Tamayo, R., Patimalla, B. and Camilli, A. (2010) Growth in a biofilm induces a hyperinfectious phenotype in *Vibrio cholerae*. *Infect Immun* **78**: 3560-3569.

- Tashima, K.T., Carroll, P.A., Rogers, M.B., and Calderwood, S.B. (1996) Relative importance of three iron-regulated outer membrane proteins for in vivo growth of *Vibrio cholerae*. *Infect Immun* **64**: 1756-1761.
- Tischler, A.D., and Camilli, A. (2004) Cyclic diguanylate (c-di-GMP) regulates *Vibrio cholerae* biofilm formation. *Mol Microbiol* **53**: 857-869.
- Touati, D. (2000) Iron and oxidative stress in bacteria. *Arch Biochem Biophys* **373**: 1-6.
- Waldor, M.K. and Mekalanos, J.J. (1994) Emergence of a new cholera pandemic: molecular analysis of virulence determinants in *Vibrio cholerae* O139 and development of a live vaccine prototype. *J Infect Dis* **170**: 278-283.
- Weaver, E.A., Wyckoff, E.E., Mey, A.R., Morrison, R., and Payne, S.M. (2013) FeoA and FeoC are essential components of the *Vibrio cholerae* ferrous iron uptake system, and FeoC interacts with FeoB. *J of Bacteriol* **195**: 4826-4835.
- Wortham, B.W., Oliveira, M.A., Fetherston, J.D., and Perry, R.D. (2010) Polyamines are required for the expression of key Hms proteins important for *Yersinia pestis* biofilm formation. *Environ Microbiol* **12**: 2034-2047.
- Wortham, B.W., Patel, C.N., and Oliveira, M.A. (2007) Polyamines in bacteria: pleiotropic effects yet specific mechanisms. *Advances in experimental medicine and biology* **603**: 106-115.
- Wyckoff, E.E., Mey, A.R., Leimbach, A., Fisher, C.F., and Payne, S.M. (2006) Characterization of ferric and ferrous iron transport systems in *Vibrio cholerae*. *J of Bacteriol* **188**: 6515-6523.

- Wyckoff, E.E., Mey, A.R., and Payne, S.M. (2007) Iron acquisition in *Vibrio cholerae*. *Biometals : an international journal on the role of metal ions in biology, Biochem, and medicine* **20**: 405-416.
- Wyckoff, E.E., and Payne, S.M. (2011) The *Vibrio cholerae* VctPDGC system transports catechol siderophores and a siderophore-free iron ligand. *Mol Microbiol* **81**: 1446-1458.
- Wyckoff, E.E., Smith, S.L., and Payne, S.M. (2001) VibD and VibH are required for late steps in vibriobactin biosynthesis in *Vibrio cholerae*. *J of Bacteriol* **183**: 1830-1834.
- Wyckoff, E.E., Valle, A.M., Smith, S.L., and Payne, S.M. (1999) A multifunctional ATP-binding cassette transporter system from *Vibrio cholerae* transports vibriobactin and enterobactin. *J of Bacteriol* **181**: 7588-7596.
- Yamamoto, S., Shinoda, S., and Makita, M. (1979) Occurrence of norspermidine in some species of genera *Vibrio* and *Beneckeia*. *Biochemical and biophysical research communications* **87**: 1102-1108.

Vita

Will Brennan III was born in Durham, North Carolina and attended Apex High school. After graduating he went to Appalachian State University in Boone, NC and graduated in 2012 with a B.S. in Biology. After receiving his M.S. in Cellular and Molecular Biology from Appalachian State University in Boone, NC in August 2015, he will pursue a career in the pharmaceutical industry.